

Spin polarization of low-energy electrons interacting with solid surfaces

S. A. Knyazev, G. K. Zyryanov, and I. A. Pchelkin

NIIF of the A. A. Zhdanov Leningrad State University

Usp. Fiz. Nauk **146**, 73–104 (May 1985)

The problems of spin polarization of low-energy electrons interacting with solid surfaces are reviewed. Special attention is paid to describing the methodology of obtaining beams of polarized electrons, methods of analyzing the spin state of the electrons in a beam, and also to the method of spin-polarized low-energy electron diffraction. Results are presented of theoretical and experimental study of the energy, angular, and temperature-dependences of the spin polarization of electrons scattered by solid surfaces, and of the effect of adsorption on the polarization of electrons for nonmagnetic and magnetic surfaces. Experiments to study the spin polarization of inelastically scattered electrons are described. In conclusion the prospects of studies involving analysis of the spin state of emitted and scattered electrons are pointed out.

TABLE OF CONTENTS

1. Introduction.....	372
2. Sources of polarized electrons.....	373
2.1 Sources of polarized electrons used in experiments with atomic beams. 2.2 Polarization of electrons in auto-, photoemission, and electron scattering by solids. Solid-state sources of polarized electrons.	
3. Analyzers of electron spin polarization.....	375
3.1 Atomic detector of spin polarization. 3.2 Diffraction detector of spin polarization. 3.3 Absorption-type detector.	
4. Spin-polarized low-energy electron diffraction.....	377
4.1 The methodology of measuring the spin polarization of electron beams. 4.2 Spin-orbit interaction in electron scattering by solids. 4.3 Spin-polarized low-energy electron diffraction from the surface of nonmagnetic crystals. 4.4 Relationship between asymmetry of scattering and polarization. Rotation diagrams. 4.5 Surface resonance scattering in spin-polarized low-energy electron diffraction. 4.6 Adsorption effects. 4.7. Temperature-dependence of the polarization. 4.8 Spin-exchange interaction in electron scattering by solids. Spin-polarized low-energy electron diffraction from the surface of magnetic materials.	
5. Spin polarization in secondary electron emission.....	386
6. Conclusion.....	388
References.....	389

1. INTRODUCTION

The general tenets on the spin polarization of electrons, polarization effects in photoelectric emission, and atomic collisions are the topic of a number of review articles.^{1–4} This review aims to treat the studies involving the spin polarization of low-energy electrons ($E_p = 0$ –1000 eV) arising from their interaction with solid surfaces. The review pays its attention to describing methods of obtaining polarized electrons (PEs) and methods of determining the degree of polarization of the electrons in a beam, as well as discussing the polarization effects that arise in elastic and inelastic scattering of electrons by solids.

The first attempt to detect polarization of electrons was undertaken by Davisson and Germer⁵ in 1929, shortly after their proof of the wave properties of electrons. They studied the double reflection of low-energy electrons from a single crystal of nickel and reported that polarization is not observed. Analogous results were also obtained by other investigators.^{6,7}

In the same year Mott⁸ studied the problem of scattering of electrons by the Coulomb field of nuclei and found

that appreciable polarization must be observed in the scattering of fast electrons with an energy of the order of 100 keV by the nuclei of elements of high atomic number Z , and that the expected polarization is extremely small at electron velocities $v_{el} \ll c$.

The failures of the first experiments on polarization of slow electrons combined with the theoretical predictions of Mott channeled the further continuation of studies on spin polarization only toward fast electrons; it was discovered experimentally only in 1943.⁹

In 1941 Massey and Morh¹⁰ showed that polarization effects must be observed also in scattering of low-energy electrons by atoms, as was confirmed by experiments with mercury beams.¹¹ Considerable successes had been attained by the middle 60s in studying polarization effects in the collisions of electrons with atoms. In 1966 Maison¹² suggested that polarization of low-energy electrons, which had been observed in scattering by atoms, must also be observed in the scattering of electrons by solid surfaces. In fact, polarization of electrons having $E_p = 90$ –300 eV scattered from a mercury surface¹³ as well as from foils of W, Pt, and Au¹⁴ was detected.

It became evident that one must take into account the dependence of the scattering cross-section on the spin orientation of the incident electron in the theoretical and experimental study of the process of interaction of electrons with solid surfaces, and to determine the spin state of the scattered electrons along with measuring the intensity. A new method of studying surfaces arose—spin-polarized low-energy electron diffraction (SPLEED).

The initial advances in SPLEED involve the theoretical treatment of the polarization effects that arise in scattering of electrons by a crystal surface.¹⁵⁻²² The first successful SPLEED experiment was performed on tungsten.²³ Considerable progress in spin-polarization studies involved the construction of highly efficient PE sources based on GaAs.²⁴ The invention of absorptive-type spin-polarization detectors²⁵ greatly simplified the problem of determining the polarization of electrons. Study of the spin state of inelastically scattered electrons showed²⁶ that they also show spin polarization.

In this review we shall not take up in detail the fundamental concepts involved in the spin polarization of electrons—they have been presented in sufficient detail²⁷—nor the theoretical aspects of spin polarization of slow electrons, which are the topic of a separate review.²⁸ We hope that this paper will help investigators involved with emission electronics and the physics of solid surfaces in designing experiments on polarization of emitted and scattered electrons.

2. SOURCES OF POLARIZED ELECTRONS

Various methods exist for obtaining electron beams with a preferential orientation of the spins. A number of review articles have been devoted to this problem.^{29,30} We shall briefly treat the PE sources employed in experiments with atomic beams, and then take up in greater detail the results of experiments to study the polarization of electrons in auto- and photoemission and the scattering of electrons by solid surfaces from the point of view of designing solid-state PE sources.

Table I presents the different types of PE sources, indicates the method of obtaining PE, and briefly characterizes these sources.

In addition to the ordinary characteristics of beams of charged particles such as the beam intensity I and its emittance ε ,³¹ PE beams are commonly characterized by the following parameters:

- the degree of polarization P of the beam;
- the quality index ξ , defined as $\xi = P\sqrt{I}$;
- the direction of polarization of the electrons in the beam;
- the possibility of reversing the polarization.

The latter parameter is especially valuable, since PE sources with reversible polarizability considerably simplify the problem of quantitatively determining the polarization effects that arise in electron scattering. Reversal of polariza-

TABLE I. Sources of polarized electrons

Type of source	Method of obtaining	P, %	Reversal of P	Current		AE, eV	eV, mm ² , sr	Ref.	Notes
				dc, A	pulsed el/pulse				
Photoionization	Photoionization of polarized atoms by unpolarized light, Li Photoionization of unpolarized atoms by circularly polarized light (Fano effect), Cs	85	Magnetic		$2 \cdot 10^{10}$	1500	$6 \cdot 10^{13}$	32	
		63	Optical	10^{-8}		3	$4 \cdot 10^{12}$	33	
		84		$5 \cdot 10^{-9}$		> 1.5		34	
Photoemission	Photoemission from magnetized ferromagnets	54	Magnetic					39	
		58	"		$10^{18} - 10^{19}$			41	Fe film covered with Cs, $H = 10^6$ A/m, $T = 4.2$ K, $f_{\text{pulse}} = 6$ Hz, $\tau_{\text{pulse}} = 1$ μ s.
	EuO								
	Photoemission from semiconductors illuminated with circularly polarized light:								
	GaAs (100) with NEA	43	Optical	$2 \cdot 10^{-5}$		0.13	$4 \cdot 10^{12}$	24	10^{-3} W incident light
	GaAsP with NEA	49	"					55	
Autoemission	GaAs — Al _x Ga _{1-x} As with NEA	40	"	$2.5 \cdot 10^{-5}$				56	5×10^{-3} W incident light
	GaAs (110) with PEA	35	"	$4 \cdot 10^{-6}$		0.3		16	10^{-3} W incident light
	Autoemission from magnetized points at low temperature, EuS/W	85	Magnetic	10^{-8}		0.1	$2 \cdot 10^{10}$	53	
		91	"					54	
Secondary emission	Inelastic scattering of electrons by solid surfaces	70		10^{-8}				57	$H = 10^6$ A/m, $f_{\text{pulse}} = 1 - 100$ Hz, $\tau_{\text{pulse}} = 250$ μ s, $E_0 = 125$ eV, $I_0 = 100$ μ A
Impact ionization	Chemoionization of metastable He in the afterglow region upon collision with a CO ₂ gas target.	40	Optical	$2 \cdot 10^{-6}$		0.15	1.6	35	
		81		$5 \cdot 10^{-8}$					
Diffraction	Elastic scattering of unpolarized electrons by the crystalline solid surface W (001): (11) beam ¹	23	Change in scattering angle ϑ	$3 \cdot 10^{-8}$				30	$I_{\text{PE}}/I_0 = 10^{-3}$
	(00) beam	From -47 to +6	Change in E_p	$2 \cdot 10^{-7}$					$I_{\text{PE}}/I_0 = 3 \cdot 10^{-4}$

tion is carried out by changing the angle of emission or the energy of emission, by reversing a magnetic field, and by reversing the optical polarization of the radiation incident on the source that gives rise to photoionization or photoemission.

2.1 Sources of polarized electrons used in experiments with atomic beams

Experimental study of the polarization arising in scattering of electrons of energy ~ 1 keV by an atomic beam of mercury showed³¹ that at a scattering angle $\vartheta = 120^\circ$ the value of P is as much as 80%. However, with a current of the primary beam of $100 \mu\text{A}$, the PE current amounts to only 10^{-13} A. Hence the scattering of electrons by atomic beams is an ineffective method of obtaining PEs.

Photoionization of lithium atoms preliminarily polarized by passing the atomic beam through a region of inhomogeneous magnetic field has been employed in Ref. 32 to build a pulsed source of PEs with a high degree of polarization ($P = 85\%$).

A source of PEs has been described³³ based on the Fano effect. In the photoionization of unpolarized cesium atoms by circularly polarized light from a mercury-xenon lamp, flux arises of longitudinally polarized photoelectrons with a degree of polarization $P = 63 \pm 3\%$ and with a beam current $I = 10^{-8}$ A. Reversal of the polarization of the photoelectrons is carried out by reversing the polarization of the light beam. An analogous source has been described in Ref. 34.

Hodge *et al.*³⁵ have described a PE source in which metastable He atoms generated by a UHF discharge are optically pumped with circularly polarized light and chemoionized by collision with a gas target to form polarized electrons. The PE current is 2×10^{-6} A, with $P = 40\%$. The use of a laser for optical pumping enabled improving the parameters of a source of this type.³⁶

2.2. Polarization of electrons in auto-, photoemission, and electron scattering by solids. Solid-state sources of polarized electrons

According to the band model, the spin degeneracy is removed in the valence band of a magnetized ferromagnetic, and, using photoexcitation one can obtain an electron flux with 100% polarization. The initial experiments to study photoemission from Ni, Co, Fe, Gd, EuO, and EuS either yielded no polarization, or they yielded a value of P of the order of several percent.^{37,38} The outline of these experiments is as follows. A film of a ferromagnetic material is evaporated onto the bottom of a Dewar flask cooled to 4.2 K in an ultrahigh vacuum. The specimen is magnetized perpendicular to its surface in a field of the order of 10^6 A/m. Deposition of a layer of cesium on the surface of the film enables one to use light sources in the visible region of the spectrum. A more detailed description of the methodology of these experiments is given in the review of Ref. 2.

One of the first solid-state PE sources is described in Ref. 39. An electron beam with $P = 54\%$ was obtained in photoemission from a magnetized polycrystalline film of iron coated with a layer of cesium. Reference 41 describes a photoemission pulsed PE source based on an EuO crystal

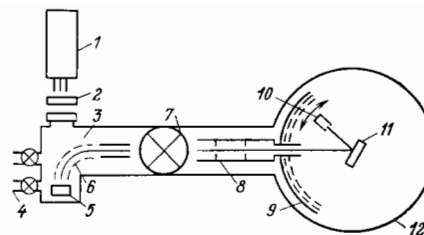


FIG. 1. Diagram of a SPLEED instrument.²⁴ 1—light source, 2— $\lambda/4$ plate, 3—photoemission source chamber, 4—sources of Cs and O_2 , 5—photocathode, 6—spherical condenser, 7—transmission valve, 8—electron gun, 9—grids and luminescent screen, 10—Faraday cylinder, 11—crystal under study, 12—LEED chamber.

doped with La.

A group of researchers in Zurich have developed a PE source based on photoemission from GaAs,⁴²⁻⁴⁴ which at present is the most developed of the polarization sources.

In the excitation by circularly polarized light of electrons from the valence band of GaAs split by spin-orbit interaction, the polarization of the photoelectrons entering the conduction band amounts to 50%. One can increase the efficiency of photoemission by producing states with a negative electron affinity (NEA) on the surface of GaAs by combined treatment of the GaAs with cesium and oxygen.

Let us examine the design of a GaAs source with NEA specially developed for experiments on SPLEED.²⁴ Figure 1 shows a block diagram of the apparatus. Light from the laser 1, which operates in a continuous regime, is circularly polarized at 2 and is incident on the (100) surface of the GaAs crystal 5. The emerging photoelectrons are deviated by 90° by the electrostatic field 6, accelerated to 1 keV and directed through the transmission valve 7 into the diffraction camera 12. The strength of the PE current depends on the intensity of the incident radiation, and in this study amounted to as much as $20 \mu\text{A}$. Owing to depolarizing effects the degree of polarization of the photoelectrons amounted to $43 \pm 2\%$. The polarization was reversed by rotating the plate 2. In the course of time the intensity of the photocurrent declined (without change in the value of P). The photocurrent was restored by heating the photocathode, with deposition of a new portion of cesium on the surface of the GaAs.

We note that Refs. 45-46 treated the depolarizing effect of the layers of Cs and O_2 , which created an NEA state on the surface of the GaAs, on the polarization of the emitted photoelectrons. They proposed a PE source based on GaAs with a positive electron affinity and having good enough working characteristics.

The use as a photocathode of epitaxial films of GaAs grown from a molecular flux made it possible to obtain PE beams with $P = 49\%$.⁴⁷

The procedure of obtaining PEs in autoelectron emission (AEE) from ferromagnetic materials is analogous in many ways to the photoemission experiments: a strong magnetic field magnetizing the emitter, low temperature to decrease the depolarization of the emitted electrons.

In the first experiments on AEE from Ni,⁴⁸ the polarization of the autoelectrons was small (from -7 to $+2\%$). Further studies showed⁴⁹ an extremely high sensitivity of the value of P of the emitted electrons to the presence of an adsorbed layer on the surface, which diminishes or completely

abolishes the polarization. In subsequent experiments⁵⁰ photoelectrons were obtained with $P = 20\text{--}25\%$, while the polarization of the emitted electrons amounted respectively to 47 and 80% upon sputtering cobalt and iron onto a tungsten point.⁵¹ Even better results were obtained for EuO and EuS on W⁵¹⁻⁵³; $P = 80\text{--}90\%$ with an emission current of 10^{-8} A. This enabled building an autoemission PE source operating in a dc regime.⁵³ Another study⁵⁴ has described a pulsed PE source based on AEE from W-EuS.

Scattering of electrons by the surface of solids consisting of heavy elements (W, Pt, Au) and magnetized by ferromagnets is also employed for obtaining PEs. With a primary-beam current of 10^{-4} A, the current of scattered electrons is 10^{-8} A. The maximum degree of polarization obtained for W and Au is $\sim 80\%$. The degree of polarization of the scattered electrons depends strongly on the cleanness of the surface—thus, for W the intensity of the polarization peaks remains invariant for several minutes in a vacuum of the order of $10^{-10}\text{--}10^{-11}$ Torr after short-term heating of a previously cleaned crystal.

Despite the variety of methods used for obtaining electron fluxes with a preferential spin orientation, it is a complex problem to obtain sufficiently intense beams with a high degree of polarization. The most widespread PE sources have been photoemission and photoionization sources, and also source employing electron scattering by atomic beams and solid surfaces. More complicated compounds: GaAsP,⁵⁵ Ga-As-Al_xGa_{1-x}As⁵⁹ have been applied as effective photoemitters in addition to GaAs.

Reference 57 is of considerable interest for the development of new PE sources, in which photoelectrons were obtained with 100% polarization from transversely magnetized Ni(001) in the absence of an external magnetic field at the instant of photoemission, as well as Ref. 58, in which polarization of photoelectrons was detected from unmagnetized W(001) illuminated with unpolarized light. It has been proposed⁵⁹ to employ the phenomenon of photoionization of atoms by circularly polarized light at the wavelength of excitation of autoionization resonances for creating PE sources of a new type. The prospects for autoemission PE sources are great. However, the low temperature of the emitting point and the large magnetic fields required for obtaining polarized beams retard the development of sources of this type.

3. ANALYZERS OF ELECTRON SPIN POLARIZATION

The classical method of determining the spin state of electrons is Mott scattering. A detailed description of the operation of a Mott analyzer²¹ is given in the review of Ref. 2. Hence we shall not spend time on it. One can find the theoretical aspects of the operation of a Mott analyzer in Ref. 60, and a description of the design in Refs. 61 and 62. New types of analyzers have been invented in recent years, such as the diffraction and the absorption analyzers. Table II shows the spin-polarization analyzers of different types, indicates the methods of analysis, and briefly characterizes these detectors.

The basis for determining the degree of polarization of a beam being analyzed is the dependence of the scattering cross-section of electrons on the orientation of their spins.

The principle of the operation of analyzers employing electron scattering consists in measuring the scattering intensity of the beam under study at the symmetric angles ϑ and $-\vartheta$: $I(\vartheta)$ and $I(-\vartheta)$. The scattering asymmetry A is defined as

$$A = \frac{I(\vartheta) - I(-\vartheta)}{I(\vartheta) + I(-\vartheta)}. \quad (3.1)$$

It depends on the degree of polarization P of the beam and the analyzing power S of the detector.³¹ This enables us to determine P from the known quantity S and the measured value of A by the relationship

$$P = \frac{1}{S} A. \quad (3.2)$$

A fundamental characteristic of analyzers is their efficiency β , which is defined as

$$\beta = \frac{A^2 I_0}{I}. \quad (3.3)$$

Here I_0 is the intensity of the incident beam, and I is the current of scattered electrons recorded by the detector.

In analyzing the spin state of electrons, one must also match the emittance of the detector and the beam being analyzed.

3.1 Atomic detector of spin polarization

As a rule, one uses a Mott analyzer as the spin-polarization detector in experiments with atomic beams. However, in experiments on double scattering of electrons by atomic beams,^{63,64} the spin polarization of the electrons scattered by the first beam is determined from the scattering by the second beam of mercury atoms. Typical parameters of the electron beams in these experiments are presented in Table II.

The low efficiency of atomic analyzers ($\sim 10^{-8}$) involves the low density of the scattering matter and the fact that the maximum polarization in atomic scattering corresponds to the minimum in scattering intensity.

In Ref. 65, the focusing of the electrons scattered by a beam of mercury atoms by a radial electrostatic field made possible a considerable increase in the intensity of the electron fluxes being detected, so that the efficiency of this type of detectors was increased up to the efficiency of solid-state analyzers.

We shall take up solid-state spin-polarization detectors in greater detail, since they are employed in experiments involving scattering of electrons by solid surfaces.

3.2 Diffraction detector of spin polarization

Kirschner and Feder⁶⁶ have employed the asymmetry of scattering of low-energy polarized electrons from materials of large Z to invent an analyzer of a new type. The diffraction detector consists of a crystal analyzer W(001) and two collectors to measure the intensity of symmetric diffracted beams. Grids are placed in front of the collectors to retard the inelastic component of scattering in the beam being analyzed, and two channel multipliers measure the intensity of the diffracted beams in a pulsed regime. Special attention must be paid to the cleanness of the surface of the crystal analyzer: the detector is located in a separate chamber in which the pressure does not exceed 4×10^{-11} Torr, and the cleanness of the W(001) surface is monitored with an Auger analyzer. The instrumental scattering asymmetry is determined by measuring the scattering intensity of an auxiliary

TABLE II. Spin polarization analyzers

Type of sonalyzer	Method of analysis	Efficiency	ε	Ref.	Notes
Mott	Measurement of the asymmetry of scattering high-energy PEs by a gold foil at symmetric angles	$10^{-5} - 10^{-4}$	300	^{61, 62}	$E_p \sim 100$ keV, scattering angles $\pm 120^\circ$, detector: Au foil.
Atomic	Measurement of the asymmetry of scattering of PEs by an atomic beam at symmetric angles	$\sim 10^{-8}$ $4 \cdot 10^{-5}$		⁶³ ⁶⁴ ⁶⁵	$E_p = 900$ eV, $\vartheta = 97,5^\circ$, $P = 0,53$ $I_0 = 10^{-4}$ A, $I = 10^{-12}$ A $E_p = 7$ eV, $\vartheta = 100^\circ$, $P = 0,39$ $I_0 = 10^{-4}$ A, $I = 10^{-11}$ A $E_p = 15$ eV, $\vartheta = 85 - 110^\circ$, $A = 0,6$, $I/I_0 \approx 10^{-4}$
Diffraction	Measurement of the asymmetry of intensity of diffraction beams of the same type in LEED patterns of W (001): (11) beam (20) beam	$1 \cdot 10^{-4}$ $8 \cdot 10^{-5}$	0,2	⁶⁷ ⁶⁸	$E_p = 70$ eV, $A = 0,21 - 0,26$ for $\Delta\vartheta = \pm 2^\circ$ $E_p = 105$ eV, $A = 0,17 - 0,21$ for $\Delta\vartheta = \pm 1^\circ$
Absorptive	Measurement of the energy of electrons being analyzed for which the SEE coefficient is $\sigma = 1$	$\sim 10^{-2}$	0,2	²⁵ ⁶⁹ ⁷¹	Detector: $Ni_{40}Fe_{40}B_{20}$ W (100) Au (110), Au Film

unpolarized beam, and also by measurements performed after the W (001) surface has been held in an atmosphere of CO and O₂, whereby the analyzing power of the tungsten crystal becomes zero.

The energy of the electrons to be analyzed and the scattering angles are chosen in such a way as to ensure an appreciable asymmetry together with a high intensity of the scattered beams. Here the scattering plane must be a plane of mirror symmetry, so that the measured magnitude A of the asymmetry equals the polarization P of the electrons being analyzed. An experimental comparison⁶⁷ has been performed of the possibilities of using two pairs of diffracted beams: (1,1) and (1,1), (2,0) and (2,0) for determining the electron spin polarization. A description of the operation of detectors of this type can also be found in Refs. 68 and 69.

3.3. Absorption-type detector

A new type of detector whose principle of operation is based on measuring the current through a target bombarded by the beam being analyzed has been proposed in Ref. 25. Owing to the dependence of the intensity of scattering of electrons on their spin orientation, the current in the target circuit determined by the difference between the fluxes incident on the surface and scattered from it depends on the spin state of the electrons in the incident beam. The correction to the scattering intensity of the electrons for their spin orientation is small. However, when the fluxes to and from the surface are equal, i.e., when the secondary electron emission coefficient is $\sigma = 1$, a change in the spin state of the incident electrons gives rise to a current in the target circuit. From its

magnitude and direction one can determine changes in the degree of polarization of the incident electron flux.

Figure 2 shows a graph of the dependence of the current flowing in the specimen on the electron energy for an unpolarized beam i_0 , a beam with $P = +100\%$, and a beam with $P = -100\%$. The values of the energy corresponding to zero current through the specimen for these beams are E_0 , $E_0(\uparrow)$, and $E_0(\downarrow)$. The difference in energy values $\Delta E = E_0(\uparrow) - E_0(\downarrow)$ depends on the angle of incidence ϑ of the beam being analyzed and serves as an index of the quality of the detector. The parameters characterizing the operation of the analyzer are E_0 , ΔE , and η , which is defined as

$$\eta = (|i(\uparrow) - i(\downarrow)|)/i_0. \quad (3.4)$$

One employs as detectors and analyzers of this type W (001) and Au (110) crystals, amorphous films of $Ni_{40}Fe_{40}B_{20}$, and polycrystalline films of Au sputtered directly in the analyzer chamber.⁷⁰⁻⁷¹

The method of determining the value of P with an ab-

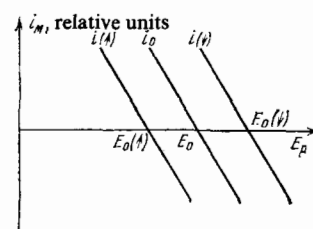


FIG. 2. Dependence of the current flowing in the target circuit on the energy of the incident electrons for different orientations of the spin of the electrons in the beam.⁷⁰

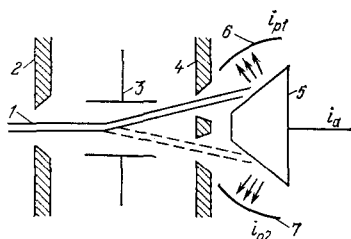


FIG. 3. Diagram of an absorptive-type detector.⁷² 1—beam being analyzed, 2—slit, 3—condenser, 4—plate with two slits, 5—analyzer prism, 6, 7—scattered-electron collectors.

sorption-type detector depends on the possibilities of reversing the polarization of the beam being analyzed, and is carried out, either by measuring the current passing through the analyzer (charge-collection method) or by measuring the energy of the beam at which the current becomes zero (zero-crossing method).

In the zero-crossing method the polarization of the beam with the reversible polarization $+P$ is determined by the relationship

$$P = \frac{E_0(+P) - E_0(-P)}{\Delta} \quad (3.5)$$

For a beam without reversal the value of P is

$$P = \frac{E_0(P) - E_0}{2} \quad (3.6)$$

For a ferromagnetic surface, one can obtain reversal of polarization by changing its direction of magnetization. For detectors whose operation is based on spin-orbit interaction, it is obtained by changing the angle of incidence of the beam on the analyzing surface from θ to $-\theta$. Figure 3 shows an original design of a detector in which the variation of the angle ϑ is carried out by the condenser 3, which directs the electron beam alternately onto the left-hand and right-hand faces of the prism analyzer 5. The degree of polarization P is determined either from the modulation of the current i_a flowing through the prism or from the difference of the currents i_p of the two collectors 6 and 7, which collect the scattered electrons.

In double-scattering experiments (Fig. 4), the first crystal is the source of polarized electrons and the second is the analyzer. The method of determining the polarization of the electrons in these experiments will be presented in Sec. 4.1.

Let us examine the comparative characteristics of the spin-polarization analyzers described above. The fundamental merit of the high-voltage Mott analyzer is the undemanding conditions for its operation. It functions successfully in a vacuum of the order of 10^{-6} Torr. Its analyzing power depends weakly on the energy of the electrons being measured and on the scattering angle ϑ . The fundamental defect of this

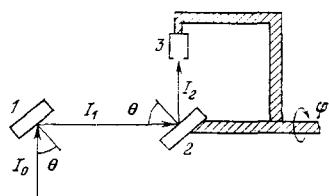


FIG. 4. Diagram of a double-scattering experiment. 1—first crystal, 2—second crystal, 3—collector.

detector is the need for using a high accelerating potential and the concomitant problem of electric insulation of the analyzer. This problem has been solved originally in Ref. 37, where a potential of the order of 120 kV is supplied to the inner cylinder of the analyzer, while its housing is grounded. The two channel multipliers recording the intensity of the electrons scattered by a gold foil have a relatively low potential with respect to ground.

The analyzing power of the Mott detector can be calculated with high accuracy. However, in measuring the polarization one must introduce a correction, not only for the instrumental asymmetry, but also for multiple scattering, which diminishes the analyzing power of the detector. Up to the present the high-voltage Mott analyzer has been successfully used to determine the degree of polarization of electron beams.⁷⁴⁻⁷⁶

The diffraction detector differs favorably from its prototype, the Mott analyzer. However, heightened requirements are imposed on the cleanness of the surface of the target analyzer, and the energy of the beam being analyzed and the scattering angles must be strictly fixed. The W (001) surface used in the diffraction detector is rapidly contaminated by residual gases. Therefore chemically more inert materials such as PbS (001)⁷⁷ have great prospects as spin-polarization detectors.

Absorption-type detectors are sensitive to the angle of incidence of the beam being analyzed, to its energy, and to the energy scatter in the beam. Therefore, these factors must be held identical during the calibration of the detector and the measurements. The surface of the detector must be shielded from adjacent insulating surfaces that might become charged by the scattered electrons and substantially alter the value of E_0 . The high efficiency, simple design, compactness, and mobility have made this type of detector the most promising in experiments on spin-polarization of low-energy electrons.

A substantial defect of all the described analyzers is that they do not measure the magnitude and direction of the polarization vector, but only its projection on one of the axes (the normal to the scattering plane or the axis of magnetization). In order to determine the vector P completely, one must successively set the axis of the detector along three mutually perpendicular axes. A method has been proposed⁷⁸ for measuring the three components of the polarization vector, while Ref. 79 has described a design for such a device.

4. SPIN-POLARIZED LOW-ENERGY ELECTRON DIFFRACTION

4.1. The methodology of measuring the spin polarization of electron beams

There are several types of devices employed in experiments with polarized electrons. In devices of the first type one measures the spin polarization that arises in the scattering of primarily unpolarized electrons by solid surfaces by using an analyzer linked with a scattering chamber.^{66,80} Figure 5 shows an apparatus of such a type. A LEED electron-optical system (2, 3) was set up on a rotating base and could be rotated about a vertical axis passing through the center of a hemispherical screen. In combination with rotation of the

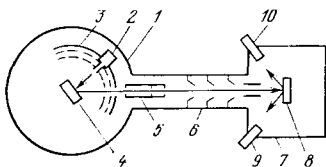


FIG. 5. Diagram of an instrument for SPLEED.⁸⁰ 1—LEED chamber, 2—electron gun, 3—grids and luminescent screen, 4—crystal, 5—electrostatic lenses, 6—acceleration system, 7—Mott analyzer chamber, 8—gold foil, 9, 10—detectors.

crystal (4), this made possible extraction of any one of the scattered beams through a slot in the luminescent screen into a second chamber (7) where the Mott analyzer was situated.

In instruments of the second type one measures the asymmetry of scattering of two electron beams of differing degrees of polarization. Figure 1 shows schematically a device of this type.²⁴ The PE source based on GaAs having NEA as described above is used in the LEED electron-optical system. When the intensity of the beams of differing polarization is equal the modulation of the intensity of the scattered electrons measured by the collector (10) at the frequency of reversal of the polarization arises from the dependence of the scattering cross-section of the electrons on the spin orientation in the incident beam. The use of a PE source allows one simply and reliably to determine the polarization effects that arise in the electron scattering.

The operation of instruments of the third type is based on the double-scattering method. In the interaction of the primarily unpolarized beam with the surface of the first crystal, the polarization of the scattered electrons is determined from the difference in intensities of reflection of electrons from the second crystal for two different positions of the latter. In essence, instruments of the first type employ one of the variants of this method. A detailed outline of the possible experiments and methods of determining the degree of polarization in double scattering has been presented in Ref. 81. Figure 4 shows the diagram of an experiment in double scattering. The collector 3 measures the intensity of the beam, which has been successively reflected from the crystals 1 and 2 as a function of the angle of rotation of the crystal 2 and the collector, which rotate as a unit about the axis of the beam I_1 . The intensity measured by the collector is determined by the relationship:

$$I_2(\varphi) = I_{20}(1 + P_1 S_2(\theta) \cos \varphi), \quad (4.1.1)$$

Here $S_2(\theta)$ is the asymmetry of scattering of the PEs by the second crystal, θ is the angle of incidence, and φ is the angle between the polarization direction and the normal to the scattering plane. With identical crystals we have $P_1 = S_2$, and the amplitude of the first harmonic as a function of $I_2(\theta)$ is determined by the quantity P_1^2 .

In the rotation-diagram method, which enables one to study the connection between the symmetry of the surface of the crystal and the vector \mathbf{P} , one measures the polarization as a function of the rotation angle of the crystal with respect to the normal to its surface, the other parameters being held constant.

A SPLEED system designed for obtaining rotation dia-

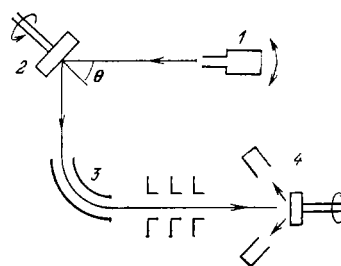


FIG. 6. Diagram of an experiment in the rotation-diagram method. 1—electron gun, 2—crystal, 3—energy analyzer, 4—Mott analyzer.

grams (Fig. 6) contains a movable electron gun (1) and a manipulator that enables one to rotate the crystal (2) about its normal. When the diffracted beam has passed through the condenser, which converts the longitudinal component of the polarization vector into a transverse component, the beam is incident on the spin-polarization detector (4), which can be rotated about the axis of the beam being analyzed.

The method has become widespread in recent time of simultaneously using a PE source and an analyzer of the scattered electrons with respect to energy and spin. This enables one to study directly effects of exchange interaction manifested in a change in the spin state of the electrons in elastic and inelastic interactions with a solid (Fig. 7).

4.2. Spin-orbit interaction in electron scattering by solids

According to the Mott model of scattering, a spin-orbit interaction arises in the motion of an electron in the field of the nucleus. The radial electric field of the Coulomb interaction of the electron and nucleus in the system of coordinates associated with the moving charge is converted into a magnetic field perpendicular to the scattering plane. This magnetic field acts on the intrinsic magnetic moment of the moving electron. If initially the spin of the incident electron is not oriented in the scattering plane, two important effects arise:

1. The magnetic field exerts an orienting action on the spin of the electron, while trying to rotate it along the direction of this field. Therefore, after scattering, initially unpolarized electrons acquire a preferential spin orientation in the direction perpendicular to the scattering plane.

2. The differential scattering cross-sections differ for electrons with the spin (\uparrow) and the spin oriented in the oppo-

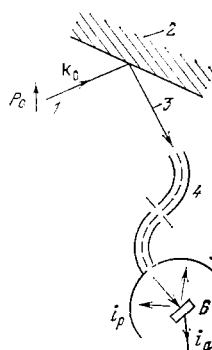


FIG. 7. Diagram of an instrument to study the exchange interaction.¹⁷² 1—primary beam, 2—specimen, 3—scattered beam, 4—energy analyzer, 5—scattered-electron collector, 6—absorptive-type analyzer.

site direction (1) with respect to the normal to the scattering plane. Consequently the symmetry of Rutherford scattering at the symmetric angles ϑ and $-\vartheta$ breaks down for a primarily polarized beam. The latter serves as the basis for determining the spin state of the electrons.

The calculations of Mott imply that an appreciable polarization owing to spin-orbit interaction must arise only in the scattering of high-energy electrons by atoms with large Z . However, the Born approximation used in these calculations ceases to hold for low-energy electrons.

The problem of scattering of electrons by atoms with the spin taken into account reduces to finding the scattering amplitude for electrons with spin oriented parallel to the normal to the scattering plane $f(\vartheta)$ and antiparallel to it $g(\vartheta)$. When expanded in partial waves, these amplitudes can be represented as

$$\begin{aligned} f(\vartheta) &= \frac{1}{2ik} \sum_l [(l+1) \exp(2i\delta_l^+ - 1) + l \exp(2i\delta_l^- - 1)] P_l(\cos \vartheta), \\ g(\vartheta) &= \frac{1}{2ik} \sum_l [-\exp(2i\delta_l^+) + \exp(2i\delta_l^-)] P_l^1(\cos \vartheta). \end{aligned} \quad (4.2.1)$$

Here P_l and P_l^1 are Legendre polynomials, and k is the wave vector.

The expression for the scattering intensity has the form

$$I(\vartheta) = |f(\vartheta)|^2 + |g(\vartheta)|^2. \quad (4.2.2)$$

The spin polarization P directed along the normal to the scattering plane is equal to the scattering asymmetry A , and is determined by the expression

$$P(\vartheta) = A(\vartheta) = -\frac{2 \operatorname{Im} [f(\vartheta) g^*(\vartheta)]}{I(\vartheta)}. \quad (4.2.3)$$

In atomic scattering the magnitudes of the phase shifts δ_l^+ and δ_l^- with allowance for the spin-orbit interaction are found from the solution of the Dirac equation with an appropriate choice of a model of the scattering potential. The maximal polarization effects associated with asymmetry of scattering are observed for electrons whose spin is oriented along the normal to the scattering plane. The polarization maxima correspond to the minima of scattering intensity.

Reference 82 has presented the results of detailed calculations of differential cross-sections and spin polarization of electrons scattered by atoms of different Z as functions of the scattering angle ϑ ($0^\circ < \vartheta < 180^\circ$) and the electron energy ($100 \text{ eV} < E_p < 1500 \text{ eV}$).

In the kinematic approximation, the transition to scattering of electrons by crystalline solids involves summation of the secondary waves over all the atoms in the crystal lattice:

$$\begin{aligned} F &= \sum_j f_j \exp[i(\mathbf{k}, \mathbf{r}_j)], \\ G &= \sum_j g_j \exp[i(\mathbf{k}, \mathbf{r}_j)]. \end{aligned} \quad (4.2.4)$$

Here \mathbf{r}_j is the radius vector of the j th atom in the lattice. The degree of polarization of the electrons scattered by the crystal, which is defined as $-2 \operatorname{Im} FG^* / (|F|^2 + |G|^2)$ reduces to

(4.2.3), which corresponds to the polarization that arises in scattering by a single atom.

Thus, in the kinematical approximation the energy and angular distribution of the intensity of electron scattering reflects the mutual arrangement of the atoms in the lattice, while the degree of polarization does not depend on the geometry of the crystal and is determined only by the properties of the individual atoms constituting the crystal.

The basis of the dynamical calculations of the polarization of electrons scattered by a solid is the model of the cell potential.⁸³ In the first stage one calculates the process of single scattering of electrons by the ionic framework of the crystal lattice. In the second stage one allows for the influence of multiple scattering, which considerably affects the angular and energy distribution and the polarization of the scattered electrons, for which one uses the methodology of the calculations developed in LEED.⁸⁴ The crystal is divided into layers parallel to the surface. Initially one treats scattering within one layer, then that between layers. One can find a detailed presentation of the calculations of SPLEED with allowance for multiple scattering in Refs. 15, 16, 20, 21, and 85.

The parameters varied in these calculations include the real and imaginary components of the internal potential, the magnitude of the displacement of the upper atomic layer in the direction of the normal to the surface, and the form of the potential at the crystal-vacuum boundary. These parameters substantially affect the energy and angular position of the polarization peaks. The calculations themselves are performed by the trial-and-error method. That is, the parameters are chosen to make the experimental results agree best with the calculated results.

4.3. Spin-polarized low-energy electron diffraction from the surface of nonmagnetic crystals

The following nonmagnetic crystals have been studied experimentally by the SPLEED method: tungsten, platinum, and gold, for which the theory has predicted considerable polarization effects arising from spin-orbit interaction. For crystals consisting of atoms of high Z , the characteristic SPLEED features are:

1. One observes at certain values of the electron energy and scattering angle a high degree of polarization of the scattered electrons, which indicates large differences in the scattering cross-sections for electrons with opposite orientations of the spin. Thus, for example, for a polarization peak with $P = 80\%$, the scattering cross-section of electrons with a \uparrow spin is nine times larger than for electrons with a \downarrow spin.

2. The shape and angular and energy position of the polarization peaks strongly depend on the diffraction conditions. A change in the angle of incidence of the electrons on the crystal surface by 1° or an energy shift by 1–2 eV can lead to a radical change in the polarization curves.

3. In many cases the intensity and polarization of the scattered beams are not intercorrelated—in contrast to scattering by atoms, the intensity minima do not necessarily correspond to the polarization maxima. For certain values of the energy and scattering angles in the case of adsorption or

change in the temperature of the crystal, the change of one of the characteristics (the intensity or polarization) is accompanied by a relative constancy of the other.

Now let us examine the concrete data obtained for the crystals mentioned above of W, Pt, and Au.

a) Tungsten

The greatest number of studies on SPLEED from the surface of nonmagnetic crystals has been devoted to theoretical calculations and experimental investigation of the surface of tungsten.^{19,23,66,67,80,85-94}

In the first experimental study²³ the polarization of the beams scattered by the surface W (001) lay within the range from -35% to $+37\%$. A subsequent study by the same authors⁸⁰ treated the intensity and polarization of the (00) beam in the range of angles of incidence from 10° to 18° . Values of P were obtained from $+60\%$ to -80% . References 87 and 93 have presented data on SPLEED from W (001) for a specularly reflected beam at large angles of incidence ($\theta = 47.5^\circ$).

As an example, Fig. 8 shows the energy-dependence of the intensity and polarization of the (10) beam⁸⁰ for scattering of initially unpolarized electrons by a tungsten surface, while Fig. 9 shows the variation in the energy-dependence of the scattering asymmetry of initially polarized electrons arising from changing the angle of incidence of the primary beam from 9° to 24° .⁶⁷

Detailed calculations of the angular and energy-dependence of the polarization of electrons in SPLEED from W (001) for four types of scattering potential have been presented in Ref. 92.

The data on LEED and ion scattering imply that the upper atomic plane of the (001) face of W is displaced by $\Delta = 4.5-11\%$ (see Ref. 95 and the references cited there). Calculations showed⁹² that the polarization profiles are highly sensitive to variation of Δ . A comparison of the calculated data with experiment implies that $\Delta = 7 \pm 1.5\%$ for W (001).

The effect of the form of the surface potential barrier on the scattering of low-energy polarized electrons from W (001) has been treated in Ref. 89.

b) Platinum

References 75 and 96-99 have presented the results of theoretical and experimental studies of the platinum surface

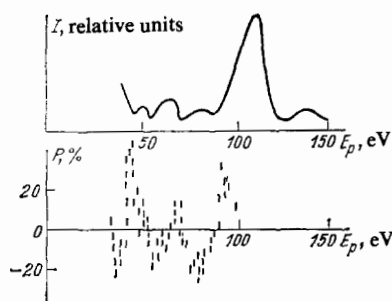


FIG. 8. Energy-dependence of the intensity and polarization of the (10) beam from W (001).⁸⁰

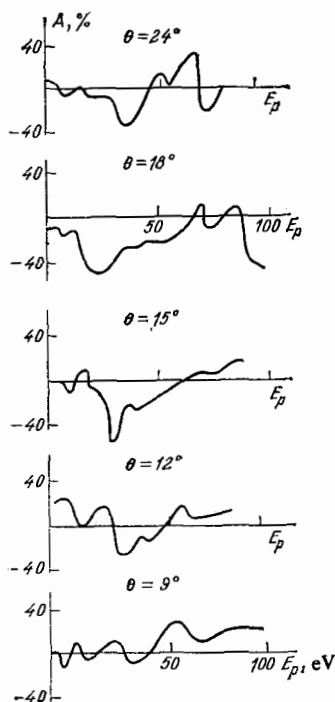


FIG. 9. Energy-dependence of the asymmetry of scattering of the (00) beam from W (001) for different values of θ .⁶⁷

by the SPLEED method. The Pt (111) surface has the structure (1×1) , and according to the data of LEED and ion scattering,¹⁰⁰⁻¹⁰² the upper atomic layer is not displaced in the direction of the normal to the surface. This enables one to compare the experimental data on polarization of scattered electrons with the calculated data, in which $\Delta = 0$ and the main attention has been paid to the shape of the surface potential barrier.

The first experimental study⁷⁵ on SPLEED from the Pt (111) surface found appreciable polarization peaks. Figure 10 shows the relationship of P to the polar angle θ for the (10) beam for the two energy values 95 eV and 85 eV. The obtained results were compared with the theoretical calculations, which used two types of scattering potential: the band-structure potential V_{b-s} and a potential with exchange interaction V_{exch} that depend on the energy, as well as two types of surface barriers: exponential and nonreflective.

We see from Fig. 10 that the theoretical calculations using the V_{exch} potential and the exponential barrier match most of the details on the polarization curves obtained experimentally.

c) Gold

A number of studies exist on the theoretical and experimental investigation of the polarization of electrons scattered from the Au (110) surface.^{68,74,96,103-110} Study of the Au (110) surface by the SPLEED method is of interest, since a reversible phase transition is observed on it. According to the LEED data,¹¹¹ a rearrangement of the (1×2) surface structure begins at $T = 650$ K, and is completed at 720 K with the formation of a (1×1) structure.

In the first experimental study on SPLEED from Au

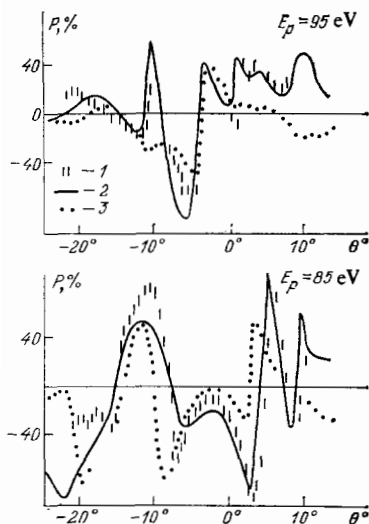


FIG. 10. Dependence of the polarization of the (01) beam on the polar angle θ of Pt (111).⁹⁷ 1—experiment, 2—scattering potential with an exchange interaction dependent on the energy, and an exponential barrier; 3—band-structure potential with an exponential barrier.

(110),¹⁰⁴ the intensity and polarization of a set of diffracted beams was studied as a function of the energy and scattering angles at $T = 710\text{--}750\text{ K}$, which corresponds to the (1×1) structure. The extreme sensitivity of the energy-dependence of the polarization of the (10) beam to small changes (within a range of 1°) in the angle of incidence of the electron beam on the gold crystal is illustrated by Fig. 11.

Figure 12 shows the $P(\vartheta)$ relationship for the (10) beam as found experimentally and the corresponding theoretical calculations of the polarization, which show the level of agreement of theory and experiment. The discrepancies of many details on the polarization curves found theoretically and experimentally can be explained by the fact that the calculations were performed for an ideal (1×1) surface structure, whereas the real surface that has undergone a phase transition contains considerable disorder.

Reference 107 has studied the $P(E)$ and $P(\vartheta)$ relationships at temperatures corresponding to the phase transition and at lower temperatures at which the structure of the Au (110) surface is (1×2) . Reference 74 and 108 have studied the asymmetry of scattering of PEs by Au (110). More detailed information on these experiments will be presented in the following sections.

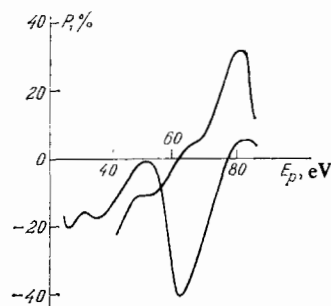


FIG. 11. Variation of the $P(E_p)$ relationship upon rotating an Au (110) crystal by 1° .¹⁰⁴

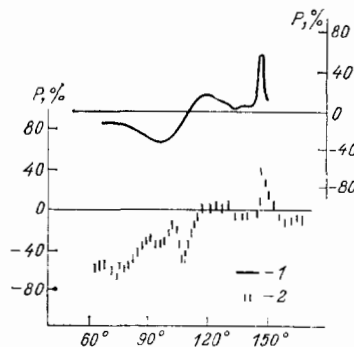


FIG. 12. Dependence of P on ϑ for the (10) beam, Au (110). 1—theory, 2—experiment.⁹⁶

4.4. Relationship between asymmetry of scattering and polarization. Rotation diagrams

The polarization that arises in scattering of an unpolarized electron beam by atoms is perpendicular to the plane of scattering and equals the asymmetry of scattering A of electrons polarized perpendicular to the scattering plane with $P = \pm 100\%$. In the scattering of electrons by a solid surface, the situation is complicated by multiple scattering and the low symmetry of the crystal surface, so that P and A are not always equal to one another.

The problems of symmetry of intensity and of P and A have been treated in theoretical studies.^{112–115} It was shown that a component of the polarization vector lying in the scattering plane arises in the scattering of electrons from a surface. The relationship between P and A is determined by the symmetry of the surface of the scattering crystal, and can be derived by studying the transformation of P and A upon time reversal. It turns out that $P = A$ when the scattering plane is a plane of mirror symmetry in the crystal.

The direct comparison of P and A has become possible with the invention of PE sources with reversible polarization.

The symmetry of scattering of PEs by the W (001) surface has been measured⁹⁰ compared with the earlier measurements of the polarization.⁸⁰ Excellent agreement was obtained between the polarization and the asymmetry of scattering curves for a specularly reflected beam at different angles of incidence.

References 74 and 108 have studied the energy and angular dependence of the scattering asymmetry for a number of diffracted beams from the Au (110) surface having the structure (1×2) . These data differ appreciably from the corresponding polarization curves.¹⁰⁴ However, subsequent SPLEED experiments on Au (110)– (1×2) with direct and reversed beams have yielded identical results. That is, they showed that $P = A$. Apparently experimental errors were introduced in Refs. 74 and 108 in determining the scattering asymmetry.

The method of rotation diagrams, which we have already described, has been used to determine the components of the polarization vector \mathbf{P} : P_n —the component normal to the scattering plane, P_k —that lying in the scattering plane in the direction along the scattered beam, and P_e —also lying in

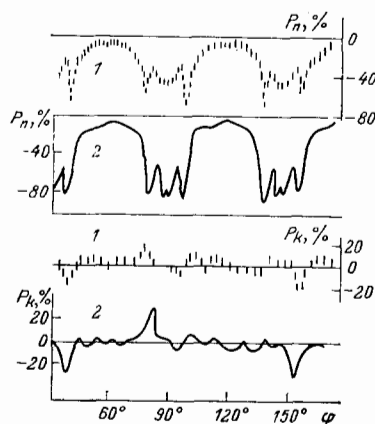


FIG. 13. Rotation diagrams of Pt (111)⁹⁷ ((00) beam, $E_p = 60$ eV, $\theta = 43.5^\circ$). 1—experiment, 2—theory.

the scattering plane and perpendicular to P_k . Figure 13 shows the results obtained experimentally and calculated theoretically for P_n and P_k in SPLEED from Pt (111).^{98,99} The component P_n is symmetric with respect to the plane of mirror symmetry of the crystal, whereas P_k is antisymmetric. The agreement between theory and experiment is very good. Figure 14 shows the dependence of the components P_n and P_e of the polarization vector on the azimuthal rotation angle of the Au (110) crystal.¹¹⁰ The component P_e , which lies in the scattering plane, is of special interest—it takes on both positive and negative values and is larger in absolute magnitude than the component P_n (in atomic scattering $P_e = 0$, and only the component P_n perpendicular to the scattering plane exists).

4.5. Surface resonance scattering in spin-polarized low-energy electron diffraction

In LEED experiments intensity peaks have been found that are explained by surface resonances. Under certain conditions an electron flux arises in the crystal that moves parallel to the surface while undergoing multiple internal reflection from the surface potential barrier. Owing to multiray interference, an intensity maximum is formed that differs in properties from the ordinary Bragg maxima. Resonance peaks arise at low electron energies.

The theoretical calculations performed for W (001) and

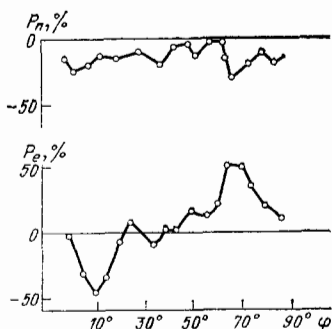


FIG. 14. Dependence of the polarization components P_n and P_e on the azimuthal angle of rotation of the Au (110) crystal¹¹⁰ ($E_p = 100$ eV, $\theta = 140^\circ$).

Ni (111)^{18,89,116,117} have shown that surface resonance scattering depends on the orientation of the spin of the incident electron. Pierce *et al.*^{118,119} have experimentally studied the resonance scattering in SPLEED from the W (001) surface. For electrons of energy 2–9 eV at angles of incidence of 15–25° in the direction of the [01] azimuth, they observed a resonance sequence of peaks whose splitting depended on the orientation of the spin of the incident electron. The calculations presented in Ref. 120 agree satisfactorily with experiment.

4.6. Adsorption effects

As a rule the polarization of low-energy electrons scattered from a gas-covered surface is zero. This is one of the ways of determining the instrumental asymmetry in the alignment of spin-polarization detectors. In a vacuum of the order of 10^{-10} Torr, the height of the polarization peaks decreases with time, and becomes zero after several hours. Hence, restoration of the initial polarization requires a repeated cleaning of the surface of the crystal being studied. However, a series of studies on the influence of adsorption of O_2 , CO, N_2 , and H_2 on W (001) in SPLEED have shown a complicated dependence of the value of P on the degree of covering of the tungsten surface with the adsorbate being studied.

The adsorption of CO and O_2 in disordered form on W (001) has been studied from the energy-dependence of the intensity and polarization of a specularly reflected beam.¹²¹ Both adsorbates strongly diminish the height of the polarization at 75 eV (the polarization declines from -75% for a clean surface to zero upon exposure of the crystal in a gaseous medium equal to 1 L). We note that the sharp variation of the polarization in the case of adsorption is accompanied by a small change in the intensity of the (00) beam. On the contrary, when $E_p = 57$ eV, the intensity of the specularly reflected beam varies severalfold without an appreciable change in its polarization.

Reference 122 has studied the effect of ordered adsorption of oxygen on the spin polarization of electrons scattered by W (001). The intensity and polarization of the specularly reflected beam were measured as functions of the energy and azimuthal angle for both superstructures $p(4 \times 1)$ and $p(2 \times 1)$ that have been observed upon adsorption of O_2 on W (001). The differences in the changes in polarization for the two superstructures indicate a different character of the reconstruction of the W (001) surface upon adsorbing O_2 in the ordered form. The authors consider that the polarization of the scattered electrons is more sensitive to the reconstruction of a surface upon adsorption than the intensity is.

The adsorption of CO on W (001) in the ordered phase has been studied by SPLEED in Ref. 123. Holding the tungsten surface in a CO atmosphere with an exposure of 20 L with subsequent heating to 1150 K gives rise to a $c(2 \times 2)$ superstructure and to a sharp positive peak at $E_p = 71$ eV. As the authors propose, desorption of CO of the β -phase occurs on heating, and the ordered $c(2 \times 2)$ structure consists of CO adsorbed in the β_3 -phase. Subsequent exposure of the system W (001)- $c(2 \times 2)$ CO in an atmosphere of carbon

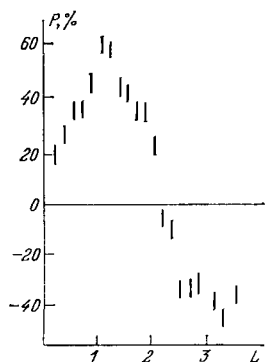


FIG. 15. Dependence of the polarization of the (00) beam on the exposure of the W (001) surface in nitrogen¹²⁴ ($E_p = 73$ eV, $\theta = 13^\circ$).

monoxide with an exposure of 2L alters the intensity of the diffraction pattern and gives rise to a broad negative polarization peak, which was proposed for designing an efficient spin-polarization analyzer.

The effect of adsorption of nitrogen on the spin polarization of electrons scattered by W (001) has been studied.¹²⁴ Just as in the case of adsorption of carbon monoxide, adsorption of nitrogen in the ordered phase yields the superstructure $c(2 \times 2)$. Figure 15 shows the pattern of the sharp change in polarization of the (00) beam as a function of the exposure of the W (001) surface in nitrogen. A strong change in P was also found upon heating a tungsten crystal exposed in nitrogen: P varies from -10% at an annealing temperature of 900 K to $+60\%$ at $T \sim 1320$ K. The substantial changes in polarization at the different stages of adsorption of nitrogen show that the polarization is highly sensitive to the state of the adsorbate on the tungsten surface.

The adsorption of hydrogen on tungsten has been studied by SPLEED¹²⁵ using a PE source. Two ordered structures $c(2 \times 2)H$ and $(1 \times 1)H$, which arise upon adsorption of hydrogen on W (001), were compared with the similar structures $c(2 \times 2)$ and (1×1) that exist on a pure tungsten surface (Fig. 16). The dependence of the scattering asymmetry $A(E_p)$ for the (01) beam on the degree of covering with hydrogen is particularly remarkable, since the considerable changes in $A(E_p)$ are accompanied by a relative constancy of the intensity curves. Since the amplitude of Coulomb scattering and the spin-orbit interaction of the electrons with hydrogen are small, the change in polarization is ascribed to a rearrangement of the tungsten atoms on the surface due to the adsorption of hydrogen.

4.7. Temperature-dependence of the polarization

In the kinematical approximation the degree of polarization of electrons reflected from the surface of a solid does not depend on the temperature of the crystal, although the intensity of LEED patterns declines sharply with increasing temperature. The thermal vibrations of the atoms of the crystal lattice, which are taken into account by the Debye-Waller factor, alter the scattering amplitude f and g in identical fashion (see Eq. (4.2.1)), so that the degree of polarization of the electrons scattered by an atom or crystal remains unchanged. Taking multiple-scattering processes into account leads to the appearance of a temperature-dependence of P .

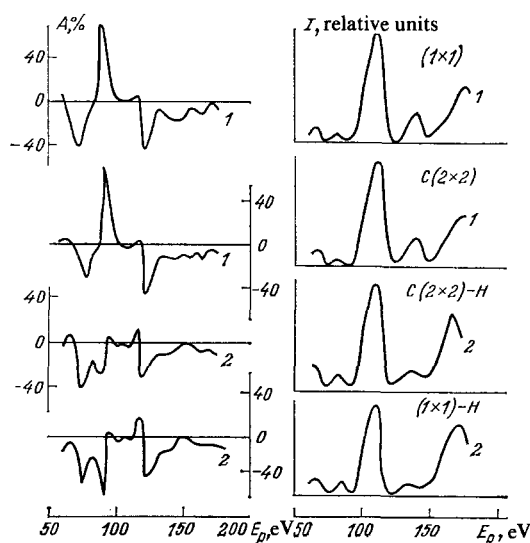


FIG. 16. Energy-dependence of the intensity and scattering asymmetry of the (01) beam at different temperatures.¹²⁵ 1—clean W (001) surface, 2—upon adsorption of hydrogen on W (001).

In this section we shall treat only the $P(I)$ relationship for clean surfaces, since the effect of temperature on the polarization of electrons scattered by a gas-covered surface was treated above, while the temperature-dependence of P for magnetically ordered structures, which involves the change in the magnetic properties of the surface with varying temperature, will be treated below.

In agreement with the kinematical theory, in the first experiment⁸⁷ on scattering of electrons from W (001), the spin polarization of the specularly reflected beam did not depend on the temperature. However, a subsequent study¹²⁶ found a substantial change in the polarization with temperature. It was found that the value of P declines with decreasing temperature for energies of electrons below that corresponding to the polarization peak, whereas for electrons of lower energy the polarization increases with declining T . Further experiments⁹³ showed that with increasing T the polarization curve shifts generally toward smaller energy, with a small change in the height of the peaks of positive and negative polarization at E_p of 70–80 eV, as is shown in Fig. 17. Theoretical calculations including multiple scattering imply that the energy shift of the polarization involves the thermal expansion of the surface lattice upon heating.

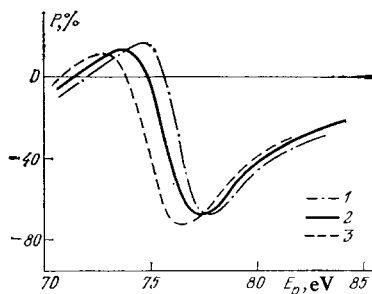


FIG. 17. Energy-dependence of the polarization of the (00) beam of W (001) at different temperatures ($\theta = 13^\circ$).⁹³ 1—350 K, 2—600 K, 3—1100 K.

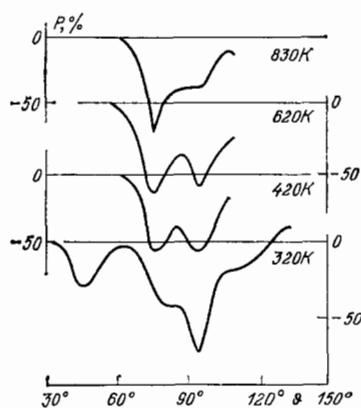


FIG. 18. Dependence of the spin polarization of the (00) beam on the scattering angle ϑ for Au (110) at different temperatures¹⁰⁷ ($E_p = 50$ eV).

Reference 125 has studied the effect of a phase transition on the spin polarization of electrons scattered by the W (001) surface. According to the LEED data, the c (2×2) structure transforms at $T \approx 350$ K to the (1×1) structure for higher temperatures. We see from Fig. 16 that the polarization curves for the (01) beam at temperatures of 100 K and 420 K differ little from one another.

In contrast to W (001), the structural phase transition on the Au (110) surface is accompanied by considerable changes in the polarization of the scattered electrons. Figure 18 shows the dependence of the polarization on the scattering angle ϑ of an electron beam specularly reflected from the Au (110) surface, as measured in the temperature range 320–830 K.¹⁰⁷ The considerable changes in the polarization curves in the region of the phase transition reflect the complicated character of the process of rearrangement of the Au (110) surface.

4.8. Spin-exchange interaction in electron scattering by solids. Spin-polarized low-energy electron diffraction from the surface of magnetic materials

Owing to the small depth of penetration of low-energy electrons into a solid (of the order of several angstroms), the SPLEED method is an ideal instrument for studying the magnetic properties of a surface: determining the magnetic moment of the upper atomic layer M_{surf} , its dependence on the magnitude of the external magnetic field H and the temperature, the presence of foreign atoms on the surface, and also the character of the change in magnetic properties from the surface to the bulk ($M_{\text{surf}} \rightarrow M_{\text{bulk}}$). In the theoretical description of SPLEED from magnetically-ordered structures, the general problems (see Sec. 4.2) are complicated by the problems of simultaneously taking into account the spin-orbit and spin-exchange interactions, the choice of the model governing the magnitude of M_{surf} , and its variation as $M_{\text{surf}} \rightarrow M_{\text{bulk}}$.

The literature contains contradictory information on the magnitude of M_{surf} and the character of the transition $M_{\text{surf}} \rightarrow M_{\text{bulk}}$.^{127–131} The initial calculations predicted substantially different spin effects in the scattering of electrons by magnetically ordered structures.^{132–137} Dynamical calculations of SPLEED by ferromagnets are highly laborious,

and the models generally employed at present are that of a homogeneous surface, in which the value of M is the same for all atomic layers, and that of the linear approximation, in which one calculates the scattering matrix $Q(M)$ only for the top atomic layer, with subsequent extrapolation of the results to the other layers M_i .¹³⁸

$$Q^{\pm}(M_i) = \frac{1}{2} [Q^+(M_{\text{surf}}) - Q^-(M_{\text{surf}})] \pm \frac{1}{2} [Q^*(M_{\text{surf}}) - Q^-(M_{\text{surf}})] M_i M_{\text{surf}}^{-1}, \quad (4.8.1)$$

Here the symbols $+$ and $-$ pertain to electrons with spins parallel and antiparallel to the axis of magnetization of the crystal.

The fundamental problem in interpreting data on SPLEED from a magnetized surface is the relation of the scattering asymmetry A (or P) to the value of M_{surf} and the character of the transition $M_{\text{surf}} \rightarrow M_{\text{bulk}}$. In the Born approximation a directly proportional relationship exists between M_{surf} and A .¹³³ Dynamic calculations with allowance for multiple scattering give rise to a more complicated relationship between A and M_{surf} :

$$A \sim \alpha M_{\text{surf}} + \beta M_{\text{surf}}^3 + \gamma M_{\text{surf}}^5 + \dots \quad (4.8.2)$$

In the general case the magnitude of M_{surf} and the character of the change $M_{\text{surf}} \rightarrow M_{\text{bulk}}$ are determined by trial and error by comparing the theoretical calculations for different values of M_{surf} with the experimental data.

If all the M_i vary in the same way with the temperature, then we have $A(T) \sim M(T)$. This case is realized for T near the Curie point (T_c), and according to the theoretical views,¹⁴⁶ we have

$$A(T) \sim M_{\text{surf}}(T) \sim \left(1 - \frac{T}{T_K}\right)^{\beta}. \quad (4.8.3)$$

There are two methods of measuring the scattering asymmetry that enable one to distinguish the contributions of spin-exchange and spin-orbit interactions.¹³⁹ If the polarization vector P_0 of the primary beam is parallel to the vector M and they both lie in the scattering plane, which is a plane of mirror symmetry of the crystal, then the contribution of the spin-orbit interaction is zero. In the second case, the vectors P_0 and M are directed along the normal n to the scattering plane. There are four methods of mutual orientation of P_0 and M with respect to one another and n that determine four scattering intensities. In a good enough approximation, the quantities A_{exch} and A_{orb} are determined from the relationships

$$A_{\text{exch}} = \frac{A^+ - A^-}{2}, \quad A_{\text{orb}} = \frac{A^+ + A^-}{2}. \quad (4.8.4)$$

Here A^{\pm} is the scattering asymmetry of PES for parallel and antiparallel magnetization of the specimen with respect to n .

Now let us examine concrete data obtained for different magnetic materials.

a) Nickel

The greatest number of studies on ferromagnetic materials by SPLEED has been devoted to nickel.^{24,117,136,138–147}

The first experiment to study the magnetization of a Ni (110) surface was presented in Refs. 140 and 141. The elastic component of the scattering asymmetry of the (00) beam was measured for $\theta = 12^\circ$ and $E_p = 125$ eV, which was of the order of 1.5%. The $A(H)$ curve had the form of a hysteresis curve. The measurements of A as a function of the temperature for $T = (0.5-0.8) T_c$ confirmed the validity of Eq. (4.8.3). A more detailed study of the $A(T)$ relationship has been presented in Refs. 144 and 145. It was found that the relationship $A \sim M_{\text{surf}}(T)$ holds over the temperature range $0.008 \leq 1 - T/T_c \leq 0.1$. The value of β is 0.82 ± 0.02 . Within the range $\pm 4\text{K}$, T_c for the surface proved to be equal to the bulk Curie temperature. Studies of $A(T)$ for Ni (001)^{145,146} have also demonstrated a linear dependence of $\ln A$ on $\ln [(1 - T/T_c)]$. The value of β is 0.79 ± 0.02 .

The value of A has been measured^{139,147} for the surface of magnetized Ni (001) with a separation of the contribution of spin-exchange and spin-orbit interaction according to the outline described above (see (4.8.4)). For the (01) beam with $E_p = 86$ eV, the values of A_{orb} and A_{exch} are very small: the mean value of A_{exch} is $\sim 1\%$ with maxima less than 2%, while A_{orb} is of the order of 2%.

The values of A_{exch} and A_{orb} for the (00) beam with $\theta = 45^\circ$ attained $\sim 10\%$ and $\sim 15\%$, respectively. A theoretical calculation of A_{exch} and A_{orb} for a very simple homogeneous model yielded good agreement with the results of experimental determination of A with subsequent separation into A_{exch} and A_{orb} .

Unmagnetized Ni was the first substance for which polarization of electrons from materials with small and medium Z was found. As we have noted in the Introduction, Davison and Germer⁵ reported failure in their experiments on double scattering of electrons from the surface of unmagnetized nickel. However, Kuyatt¹⁴⁸ in 1975 analyzed Ref. 5, and concluded that the authors had incorrectly interpreted their results and that the value of P implied by their data was $\sim 14\%$. Although Feder subsequently concluded¹¹⁷ from theoretical calculations that the observed asymmetry of scattering of electrons from the second crystal is more likely due to an inaccuracy of its positioning within the limits of 1° , the tables⁸² on spin polarization for atomic scattering imply an appreciable polarization for materials of medium Z (krypton ($Z = 36$) at $E_p = 100$ eV and $\vartheta = 96^\circ$, with $P = -11\%$, and niobium ($Z = 41$) at $E_p = 100$ eV and $\vartheta = 102^\circ$, with $P = -33\%$).

The first successful experiment on SPLEED from paramagnetic Ni was presented in Ref. 142. The asymmetry of scattering of the (00) beam ($\theta = 45^\circ$, $\varphi = 0^\circ$) from Ni (001) heated to $T > T_c$ amounted to several percent, with maxima $\sim 15\%$. The theoretical calculations of the contribution of spin-orbit interaction to $A(E_p)$ yielded good enough agreement with experiment. A subsequent paper¹⁴⁹ studied the surface of unmagnetized Ni (001) at room temperature. Supplementary experiments employing the Kerr effect showed that at T_{room} the electron beam covers a large number of differently oriented domains. Hence the effects of the exchange interaction that arise in the scattering of electrons by individual domains mutually cancel. The variation of $P(E_p)$

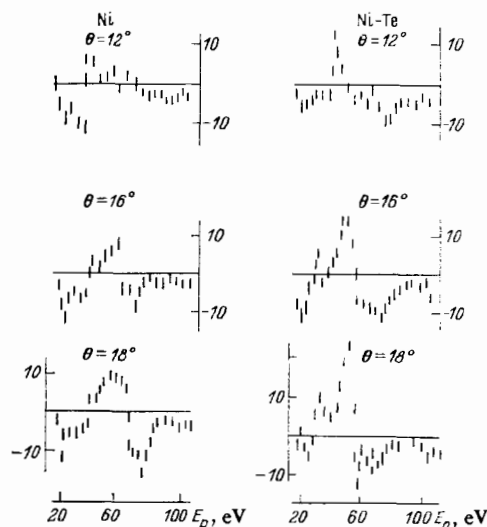


FIG. 19. The $P(E_p)$ function of the (00) beam for Ni (001) and Ni (001) with (2×2) Te¹⁴⁹ (azimuthal angle 45°).

for the (00) beam with different angles of incidence and for the (10) beam proved very sensitive to the scattering geometry and the energy of the incident electrons, as shown in Fig. 19. The observed polarization lay within the range 10–15% with a maximum value of the order of 28%.

Above we have treated the effect of adsorption of light gases on the polarization of electrons scattered by the heavy tungsten (see Sec. 4.6). The converse situation has been described in the same paper,¹⁴⁹ where the polarization effects were studied that arise in the adsorption of the heavy tellurium ($Z = 52$) on the surface of unmagnetized Ni (001) ($Z = 28$). As we should expect, the adsorption of Te on Ni (001) having the $c(2 \times 2)$ structure altered the $P(E_p)$ curves, while the values of P of the scattered electrons increased (see Fig. 19). Satisfactory agreement was obtained between the experimental data and the theoretical calculations of P , which were performed for the first time for an adsorbate-substrate system.

b) Iron

The results of theoretical and experimental study of the Fe (001) and (110) surfaces by SPLEED have been presented in Refs. 81, 132–135, 138, and 150–152. The initial calculations of the asymmetry of scattering of PES carried out in the Born approximation have yielded substantially differing results. (Thus, according to Ref. 132, the magnitude of A is $\sim 86\%$, whereas in Ref. 133 it equals only 3.5%). Further dynamical calculations¹³⁸ have shown the high sensitivity of the polarization curves to the choice of the value of M_{surf} , and have predicted considerable polarization effects in the scattering of electrons by a magnetized iron surface.

The first experimental study of SPLEED from Fe (110)^{151,152} treated films 80 layers thick grown on a W (110) surface. (This permitted relatively easy magnetization of the Fe film and elimination of the influence of scattered magnetic fields.) The maximal value of A for the (00) beam amounted to $(34 \pm 10)\%$ ($\theta = 31^\circ$, $E_p = 46$ eV). Figure 20 shows the

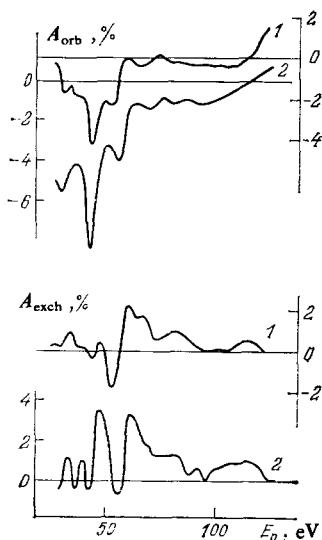


FIG. 20. Energy-dependence of the spin-orbit and spin-exchange asymmetry of scattering of Fe (110). 1—experiment,¹⁵¹ 2—theory.¹⁵⁰

results of experimental separation of A_{orb} and A_{exch} according to the outline presented above, and of the theoretical calculations of A_{orb} and A_{exch} employing the model of the linear approximation with the value $M_{\text{surf}} = 1.3 M_{\text{bulk}}$. We see that the agreement between experiment and theory is good.

c) Amorphous ferromagnets

The analysis of the polarization effects that arise in scattering of electrons by a crystal surface is complicated by diffraction. Hence the study of the surface of amorphous ferromagnetic is of undoubted interest. In Refs. 26 and 153 the asymmetry of scattering of PES from the surface of the ferromagnetic glass $\text{Fe}_{40}\text{Ni}_{40}\text{B}_{20}$ was determined. It was found that the value of A approximately does not depend on the orientation of the primary beam with respect to the surface for a fixed scattering angle ($\vartheta = 166^\circ$). Measurements of the asymmetry of elastic scattering in the range $E_p = 2\text{--}300\text{ eV}$ and $\vartheta = 166^\circ$ showed that the value of A depends in a complicated way on E_p (A changes sign twice, while reaching maximal values of -1.5% in the region of 20 eV and $+3\%$ in the region of 90 eV).

References 154 and 155 have studied in detail the polarization effects that arise in scattering of electrons by the ferromagnetic glasses $\text{Fe}_{40}\text{Ni}_{40}\text{B}_{20}$ and $\text{Fe}_{81.5}\text{B}_{14.5}\text{Si}_4$. Figure 21 compares the data for these substances and the results obtained for Fe (001). For the single crystal iron surface one observes clearly marked diffraction effects, whereas the data obtained for the two glasses are close to one another. An analysis of the obtained results implies that the spin effects that arise in scattering of electrons by amorphous ferromagnetic substances can be treated from the standpoint of scattering by a single atom corrected for the losses caused by plasmons and the creation of electron-hole pairs.

d) Nickel oxide

The very first experiment to study the exchange interaction was performed in 1968 by ordinary LEED methods.¹⁵⁶

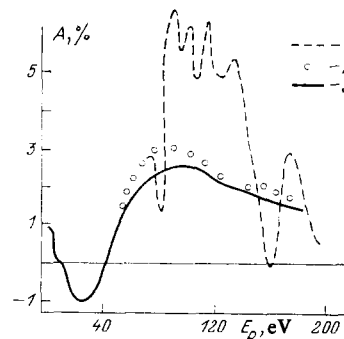


FIG. 21. $A(E_p)$ variation for a Fe (001) crystal and two ferromagnetic glasses.¹⁵⁴ 1—Fe (001), (00) beam, angle of incidence 7° ; 2— $\text{Fe}_{40}\text{Ni}_{40}\text{B}_{20}$; 3— $\text{Fe}_{81.5}\text{B}_{14.5}\text{Si}_4$, angle of incidence 0° , scattering angle $\vartheta = 166^\circ$.

In studying the LEED patterns from the surface of the anti-ferromagnet NiO (001), disappearance of reflection with half-integral indices was observed at the Néel temperature. Since the primary beam used in this study was unpolarized, the scattered electrons were also unpolarized, since the total magnetization of the Ni and O sublattices is zero.

Reference 157 presented the results of dynamical calculations of LEED from NiO (001) for different models of the exchange potential. The effects of spin polarization in SPLEED from the NiO (111) surface are discussed in Ref. 137 (the (111) surface consists of atoms of one type having identical spin orientation). Detailed studies of the temperature-dependence of the intensity of the LEED patterns of NiO (001) near the Néel temperature have made possible the determination of the character of the change in the magnetization of the Ni and O sublattices with the temperature.¹⁵⁸ It turned out that the intensity of reflections arising from the exchange interaction, i.e., the change in the magnetization of the sublattices, varies as $(T_n - T)^\beta$. The value of β is 0.89 ± 0.02 , which is somewhat higher than the theoretical predictions implied by the Ising model (0.67) and the Heisenberg model (0.75).

5. SPIN POLARIZATION IN SECONDARY ELECTRON EMISSION

The development of studies on secondary electron emission (SEE) has proceeded from measuring the SEE coefficient σ (σ is the result of integrating the distribution of secondary electrons (SEs) $f(E, \Omega)$ over the energy and the angle of emergence) to studying the energy distribution of the SEs (which has allowed classifying the SEs into truly secondary, and elastically and inelastically scattered electrons), and finally, to measuring the energy distribution of the SEs emerging at a definite angle, i.e., $f(E, \Omega)$. The studies of $f(E, \Omega)$ showed that these relationships have a complex structure and that the $f(E, \Omega)$ curves measured for different scattering angles can differ considerably from one another. The problem of the spin polarization of SEs arose in interpreting the fine structure of the $f(E, \Omega)$ spectra obtained from W (001). In Ref. 159 this structure is explained by spin effects and it is proposed that spin polarization exists in the SEs owing to the spin-orbit interaction. Thus a new method has arisen for studying surfaces—polarization secondary-electron spec-

troscopy (PSES),¹⁶⁰ which enables one to perform a complete analysis of SEs, in energies, angles, and spin.

Calculations of the spin polarization of elastically and inelastically scattered electrons require a detailed treatment of the spin-dependence of the different mechanisms of inelastic losses, which has been presented in a set of theoretical papers.¹⁶¹⁻¹⁶⁹ We shall not take up in detail the description of these calculations, but shall note schematically only the fundamental results.

The most important types of interactions leading to energy losses in electron scattering are the electron-phonon and electron-magnon interactions and the excitation of plasma oscillations and electron-hole pairs. The electron-phonon interaction is small in the SPLEED energy region and does not depend on the spin. The electron-magnon interaction for magnetically ordered structures depends on the spin and is manifested at low energies (~ 10 eV).¹⁶¹⁻¹⁶³ The contribution of plasma oscillations to inelastic scattering exhibits a weak spin-dependence, even for magnetized ferromagnets.¹⁶⁴ The process of excitation of electron-hole pairs, which is the most important mechanism of spin polarization in secondary-electron emission from ferromagnets, has been treated in a set of studies.^{165,166} The calculations of spin polarization have been performed under the assumption that a primary electron with $E_p < 50$ eV can interact only with electrons of the ferromagnet having the opposite spin orientation.¹⁶⁷ While the first calculations for Fe and Ni treated the excitation of the 3d electrons, currently the main attention is being paid to excitation of the electrons of the lattice core, i.e., the 3p electrons for Fe and Ni.¹⁵⁰

Even the first experiment on spin polarization of SEE from an unmagnetized Au (110) surface¹⁷⁰ made it possible to test a very simple model of SE formation. Figure 22 shows the energy-dependence of the spin polarization of the SEs for two scattering angles, which was compared with the calculations based on the model of two-stage scattering. In the scattering of primary electrons by a conduction electron (elastic collision of two spheres), the scattering angle ϑ_1 is unambiguously related to the energy of the electrons after collision. In the second event of elastic scattering of an electron by the ionic core of the crystal lattice through the angle ϑ_2 ($\vartheta_1 + \vartheta_2 = \vartheta$ is the measured scattering angle), a spin polar-

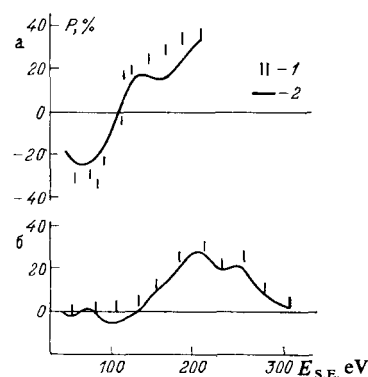


FIG. 22. Energy distribution of the polarization of secondary electrons from Au (110)¹⁷⁰ ($E_p = 600$ eV). a— $\vartheta = 139^\circ$, b— $\vartheta = 90^\circ$; 1—experiment, 2—theory.

ization of the SE arises, whose magnitude is found from the tables for atomic scattering by Au. The high level of agreement of the model calculations and experiment allows one to consider that the fundamental mechanism of formation of SEs in the studied energy region is two-stage in type.

In their next study¹⁷¹ the same authors measured two components of the spin polarization of the SEs— P_e , which lies in the scattering plane, and P_n , which is perpendicular to it. They found a considerable longitudinal component of the spin polarization, whose magnitude depended on the energy of the SEs. They found that the profiles $P_n(E_{SE})$ and $P_e(E_{SE})$ remain invariant upon changing the energy of the primary beam over the range 400–1000 eV and varying the angle of incidence, provided that the total scattering angle is conserved.

In Ref. 172 the exchange polarization P_{exch} was measured of the electrons inelastically scattered by an Au (110) surface with a primary-electron energy $E_p = 500$ eV and the initial polarization P_0 . It was found that the ratio P_{exch}/P_0 measured for SEs of energy $0.1 \leq E_{SE}/E_p \leq 0.2$ is maximal for SEs of minimal energy, and declines rapidly with increasing E_{SE} . The obtained results are treated on the basis of a simple model of single collision of the primary electron with a conduction electron of gold.

The first study on spin polarization of SEs from magnetically ordered structures was carried out for $Ni_{40}Fe_{40}B_{20}$.²⁶ Figure 23 shows a graph of the $P(E_{SE})$ relationship. As we see, the degree of polarization declines with decreasing E_{SE} , changes sign, and vanishes for true secondary electrons.

In contrast to these results, the measurements of spin polarization in the case of scattering of primarily polarized electrons by the magnetized amorphous ferromagnet $Fe_{81.5}B_{14.5}Si_4$,^{155,173} analogously to the photoemission data,¹⁷⁴ showed that the maximum polarization is observed for the true secondary electrons. Thus, for $Fe_{81.5}B_{14.5}Si_4$ with $E_p = 500$ eV, the SEs with $E_{SE} < 0.5$ eV have $P \approx 25\%$, while for SEs of energy 25 eV we find $P \approx 7\%$. The degree of polarization of the SEs of minimal energy exactly corresponds to the spin polarization of the electrons in the conduction band. Reference 173 has noted the possible use of spin polarization in SEE for constructing a scanning spin microscope.

In analogous experiments^{175,176} performed for a magnetized Ni (110) surface, the character of the variation of $P(E_{SE})$ is as before, although the value $P_{max} \approx 17\%$ obtained for the SEs of minimal energy proved to be considerably larger than the mean polarization of the electrons in the con-

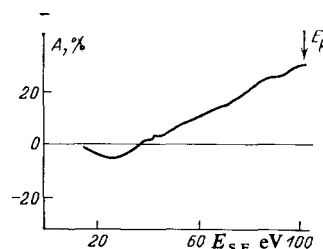


FIG. 23. Energy-dependence of the asymmetry of scattering of secondary electrons from $Ni_{40}Fe_{40}B_{20}$ ($E_p = 97$ eV, $\vartheta = 166^\circ$).²⁶

duction band of Ni (110) ($\sim 5.5\%$), while a series of maxima and minima was distinctly manifested on the dropoff of the $P(E_{SE})$ relation. Both a general decline in the polarization of the SEs and a change in the positions of the maxima and minima on the $P(E_{SE})$ curves occur in the case of adsorption of oxygen and cesium on the nickel surface.

6. CONCLUSION

Study of the spin polarization combined with measurements of the energy and angular distribution of the electrons enables one to obtain full information on the electrons scattered by a solid surface. The additional information on the change in the spin state of the electrons resulting from interaction with the material has made it possible to examine on a new, higher level the problem of interaction of electrons with a solid, and to test models describing the geometric and electronic structure of the surface.

One can say that factual material on the spin-polarization effects that arise in the reflection of electrons from a solid surface is being actively accumulated at present. However, the set of studied materials is as yet restricted. These are the three representatives of materials of high atomic number Z : tungsten, platinum, and gold, the ferromagnets Ni and Fe, the ferromagnetic glasses $Fe_{40}Ni_{40}B_{20}$ and $Fe_{81.5}B_{14.5}Si_4$, the antiferromagnet NiO, and layers of Te adsorbed on Ni. Apparently this set will expand considerably in the very near future, not only in the region of materials of high Z , but also with medium Z , since it is already possible to measure the asymmetry of scattering of polarized electrons in the range 1–3% with an accuracy amounting to fractions of a percent.

The first SPLEED experiments have already shown the high sensitivity of the polarization curves to change in the scattering angle, the energy of the incident electrons, and the cleanness of the surface being studied. This has facilitated considerable progress in the technique of polarization experiments as compared with the standard LEED methodology.

The theoretical calculations of the angular and energy dependence of the polarization of scattered electrons have also demonstrated the extreme dependence of the calculated curves on the choice of the model of the scattering potential, the magnitude of the displacement of the upper layer of the surface, the shape of the surface potential barrier, etc. However, the comparison of the calculated data with experiment in SPLEED is carried out by the trial-and-error method. That is, one selects the parameters for the calculation that yield the best agreement with experiment.

The fundamental difficulties in describing the scattering of electrons by a solid involve taking into account multiple scattering and inelastic interaction. In dynamical SPLEED calculations, multiple scattering is taken into account in two stages—in intralayer and interlayer scattering. In contrast to atomic scattering, it gives rise to a component of the vector \mathbf{P} lying in the scattering plane. Therefore, from the standpoint of manifesting the role of multiple scattering in the interaction of electrons with a solid, experiments are of undoubted interest in which one determines both the compo-

nent of the vector \mathbf{P} perpendicular to the scattering plane and that lying in it, and experiments to study the system of a "heavy" layer of adsorbate on a "light" substrate, as was first performed for the system of Ni (110) with (2×2) Te, and studies on amorphous and polycrystalline materials.

A rather detailed description exists of the dependence of the different mechanisms of inelastic interaction on the spin state of the electrons, although there are as yet few experimental studies along this line. Apparently the detailed study of these mechanisms will require further development of the methodology of experimentation.

Thus, the determination of the dispersion of the surface magnons responsible for the temperature-dependence of the surface magnetization of ferromagnets requires considerably better energy resolution of the PEs than that now existing. It is of considerable interest to compare the energy-dependence of the polarization of the inelastically scattered electrons with features on the energy distribution of the SEs, since the appearance of such features involves turning on a new mechanism of inelastic losses. Improvement of the figure of merit of PE sources would stimulate the development of studies along this line.

The tungsten-light gases system has proved to be a rather complex object for studying adsorption processes by the SLEED method, since the adsorption of gases is accompanied by reconstruction of the tungsten surface. One can already say that the specific features of adsorption of foreign atoms on a crystal surface as revealed by the LEED method is more complicated in character and does not encompass the entire kinetics of the process, since in SPLEED one observes an inadequate alteration of the intensity and polarization curves upon adsorption. The system of a heavy adsorbate on a light substrate opens up extensive possibilities for studying polarization effects arising in scattering of electrons by a monolayer of a material. Experiments to study condensed systems that do not reconstruct the surface, such as noble gases on a cold substrate, seem to promise much.

Studies of recent years have shown that the polarization of emitted electrons is completely general in character. Beams of polarized photoelectrons have been obtained from magnetized ferromagnets, from crystals of the cubic system illuminated with circularly polarized light, and finally, from nonmagnetic crystals upon illumination with unpolarized light. Electron beams with a considerable degree of polarization arise in autoelectron emission (AEE) from ferromagnets. The suggestion has been advanced¹⁷⁷ of possible AEE of spin-polarized electrons from nonferromagnetic materials. Reference 178 is of considerable interest, in which a strong effect of auxiliary illumination on the polarization of the emitted electrons was found in the study of AEE. Conditions have been found^{179–181} under which polarization of Auger electrons is possible. This has been found experimentally¹⁸² in studying the magnetized ferromagnetic glass $Fe_{83}B_{17}$.

A new method of study has appeared that combines photoemission with the interaction of polarized electrons with a solid-inverse photoelectron spectroscopy^{183,184} in which one studies the radiation arising in the bombardment of a surface with a beam of PEs. This enables one to get

information on the structure of the energy bands and the spin-dependence of the matrix elements of the transition of the electrons in the solid. The dependence of the degree of polarization of the light radiation on the polarization of the bombarding electrons offers a possibility for constructing PE analyzers of a new type.

In another method—spin-polarized electron-capture spectroscopy,^{185,186} one studies the capture of a polarized electron by a deuteron (nucleus of a deuterium atom) in the glancing reflection of deuterons from a solid surface according to the reaction: $D^+ + e = D^0$. Interesting data have been obtained on the ferromagnetism of the upper atomic layer of the antiferromagnet chromium.

A new methodology has been proposed in recent years—diffraction of slow spin-polarized positrons.^{187,188}

¹The emittance ϵ characterizes the possibility of transmission of the beam through the electron-optical system: $\epsilon = E_p S \Omega$, where E_p is the energy of the electrons, S is the area of the cross-section of the beam, and Ω is the solid angle within which the beam propagates.

²In a Mott detector the beam to be analyzed is accelerated to 100 KeV and directed onto a gold foil. The degree of polarization of the electrons is determined from the readings of two detectors lying at angles of $\pm 120^\circ$ and measuring the intensity of scattering of the electrons by the Au foil (see below, Fig. 5).

³The analyzing power S of a detector equals the polarization P of a primarily polarized beam that arises upon scattering of the electrons by the surface of the detector.

¹Kh. Tol'khuk, Usp. Fiz. Nauk **63**, 761 (1957).

²A. B. Vaganov, Usp. Fiz. Nauk **119**, 257 (1976) [Sov. Phys. Usp. **19**, 481 (1976)].

³N. B. Delone and M. V. Fedorov, Usp. Fiz. Nauk **127**, 651 (1979) [Sov. Phys. Usp. **22**, 252 (1979)].

⁴G. F. Drukarev and V. D. Ob'edkov, *ibid.*, p. 621 [Sov. Phys. Usp. **22**, 236 (1979)].

⁵C. J. Davisson and L. M. Germer, Phys. Rev. **33**, 760 (1929).

⁶A. F. Joffe and A. N. Arsenieva, C. R. Acad. Sci. **188**, 152 (1929).

⁷G. O. Langstroth, Proc. R. Soc. London Ser. A **136**, 558 (1932).

⁸N. F. Mott, *ibid.* **124**, 425 (1929).

⁹C. G. Shull, C. T. Chase, and F. E. Myers, Phys. Rev. **63**, 29 (1943).

¹⁰H. S. W. Massey and C. B. O. Mohr, Proc. R. Soc. London Ser. A **177**, 341 (1941).

¹¹R. Kollath, Z. Phys. Ser. B **5**, 66 (1949).

¹²D. Maison, Phys. Lett. **19**, 654 (1966).

¹³W. Eckstein, Z. Phys. **203**, 59 (1967).

¹⁴R. Loth, *ibid.*, p. 66.

¹⁵R. Feder, Phys. Status Solidi B **46**, K31 (1971).

¹⁶R. Feder, *ibid.* **49**, 699 (1972).

¹⁷R. Feder, *ibid.* **56**, K43 (1973).

¹⁸R. Feder, *ibid.* **62**, 135 (1974).

¹⁹R. Feder, Phys. Rev. Lett. **36**, 598 (1976).

²⁰P. J. Jennings, Surf. Sci. **20**, 18 (1970).

²¹P. J. Jennings, *ibid.* **26**, 509 (1971).

²²P. J. Jennings, Jpn. J. Appl. Phys. Suppl. **2**, Part 2, 661 (1974).

²³M. R. O'Neill, M. Kalisvaart, F. B. Dunning, and G. K. Walters, Phys. Rev. Lett. **34**, 1167 (1975).

²⁴D. T. Pierce, R. J. Celotta, G.-C. Wang, W. N. Unertl, A. Galejs, C. E. Kuyatt, and S. R. Mielczarek, Rev. Sci. Instrum. **51**, 478 (1980).

²⁵D. T. Pierce, S. M. Girvin, J. Unguris, and R. J. Celotta, *ibid.* **52**, 1437 (1981).

²⁶H. C. Siegmman, D. T. Pierce, and R. J. Celotta, Phys. Rev. Lett. **46**, 452 (1981).

²⁷J. Kessler, *Polarized Electrons*, Springer-Verlag, Berlin, 1976.

²⁸R. Feder, J. Phys. C **14**, 2049 (1981).

²⁹G. Baum, AIP Conf. Proc. **69**, Part 2, 785 (1980).

³⁰R. J. Celotta and D. T. Pierce, Adv. At. Mol. Phys. **16**, 101 (1980).

³¹K. Jost and J. Kessler, Phys. Rev. Lett. **15**, 575 (1965).

³²M. J. Alguard, J. E. Clendenin, R. D. Ehrlich, V. W. Hughes, K. P. Schuler, G. Baum, W. Raith, R. H. Miller, and W. Lysenko, Nucl. Instrum. Methods **163**, 29 (1979).

³³P. F. Wainwright, M. J. Alguard, G. Baum, and M. S. Lubell, Rev. Sci. Instrum. **49**, 571 (1978).

³⁴R. Möllenkamp and U. Heinzmann, J. Phys. E **15**, 692 (1982).

³⁵L. A. Hodge, F. B. Dunning, and G. K. Walters, Rev. Sci. Instrum. **50**, 1 (1979).

³⁶L. G. Gray, K. W. Giberson, C. Cheng, R. S. Keiffer, F. B. Dunning, and G. K. Walters, *ibid.* **54**, 271 (1983).

³⁷G. Busch, P. Campagna, and H. C. Siegmman, Phys. Rev. Lett. **22**, 597 (1969).

³⁸G. Busch, P. Campagna, and H. C. Siegmman, J. Appl. Phys. **41**, 1044 (1970).

³⁹G. Busch, P. Campagna, and H. C. Siegmman, Phys. Rev. B **4**, 746 (1971).

⁴⁰G. Busch, P. Campagna, D. T. Pierce, and H. C. Siegmman, Phys. Rev. Lett. **28**, 611 (1972).

⁴¹E. Garwin, F. Meier, D. T. Pierce, K. Sattler, and H. C. Siegmman, Nucl. Instrum. Methods **120**, 483 (1974).

⁴²D. T. Pierce, F. Meier, and P. Zürcher, Phys. Lett. A **51**, 465 (1975).

⁴³D. T. Pierce, M. Meier, and P. Zürcher, Appl. Phys. Lett. **26**, 670 (1975).

⁴⁴D. T. Pierce and F. Meier, Phys. Rev. B **13**, 5484 (1976).

⁴⁵M. Erbudak and B. Reihl, Appl. Phys. Lett. **33**, 584 (1978).

⁴⁶B. Reihl, M. Erbudak, and D. M. Campbell, Phys. Rev. B **19**, 6358 (1979).

⁴⁷S. F. Alvarado, F. Ciccacci, S. Valeri, M. Campagna, R. Feder, and H. Pleyer, Z. Phys. Ser. B **44**, 259 (1981).

⁴⁸N. Müller, Phys. Lett. A **54**, 415 (1975).

⁴⁹M. Landolt, M. Campagna, and B. Wilkens, Phys. Rev. Lett. **39**, 568 (1977).

⁵⁰M. Landolt and M. Campagna, *ibid.* **40**, 1401 (1978).

⁵¹G. Chrobok, M. Hofmann, G. Regenfus, and R. Sizmann, Phys. Rev. B **15**, 429 (1977).

⁵²G. Baum, E. Kisker, *et al.*, Appl. Phys. **14**, 149 (1977).

⁵³E. Kisker, G. Baum, A. H. Mahan, W. Raith, and B. Reihl, Phys. Rev. B **18**, 2256 (1978).

⁵⁴N. Müller, W. Eckstein, W. Heiland, and W. Zinn, Phys. Rev. Lett. **29**, 1651 (1972).

⁵⁵D. Conrath, T. Heindorff, A. Hermann, N. Ludwig, and E. Reichert, Appl. Phys. **20**, 155 (1979).

⁵⁶S. F. Alvarado, F. Ciccacci, and M. Campagna, Appl. Phys. Lett. **39**, 615 (1981).

⁵⁷E. Kisker, W. Gudat, E. Kuhlmann, R. Clauber, and M. Campagna, Phys. Rev. Lett. **45**, 2053 (1980).

⁵⁸J. Kirschner, R. Feder, and J. F. Wendelken, *ibid.* **47**, 614 (1981).

⁵⁹N. A. Cherepkov, J. Phys. B **10**, L653 (1977).

⁶⁰G. Holzwarth and H. J. Meister, Nucl. Phys. **59**, 56 (1964).

⁶¹J. Van Klinken, *ibid.* **75**, 161 (1966).

⁶²J. S. Grenberg, D. P. Malone, *et al.*, Phys. Rev. **120**, 1393 (1960).

⁶³H. Deichsel and E. Reichert, Z. Phys. **185**, 169 (1965).

⁶⁴H. Deichsel, E. Reichert, and H. Steidl, *ibid.* **189**, 212 (1966).

⁶⁵K. Jost, F. Kaussen, and J. Kessler, J. Phys. E **14**, 735 (1981).

⁶⁶J. Kirschner and R. Feder, Phys. Rev. Lett. **42**, 1008 (1979).

⁶⁷G. C. Wang, R. J. Celotta, and D. T. Pierce, Phys. Rev. B **23**, 1761 (1981).

⁶⁸N. Müller, Int. Rept. IIP 9/23 MPI, Garching, Munich, 1979.

⁶⁹M. Erbudak and N. Müller, Appl. Phys. Lett. **38**, 575 (1981).

⁷⁰R. J. Celotta, D. T. Pierce, H. C. Siegmman, and J. Unguris, *ibid.*, p. 577.

⁷¹M. Erbudak and G. Ravano, J. Appl. Phys. **52**, 5032 (1981).

⁷²H. C. Siegmman Europhys. News **14**, 9 (1983).

⁷³L. A. Hodge, T. J. Moravec, F. B. Dunning, and G. K. Walters, Rev. Sci. Instrum. **50**, 5 (1979).

⁷⁴B. Reihl, and B. I. Dunlap, Appl. Phys. Lett. **37**, 941 (1980).

⁷⁵P. Bauer, R. Feder, and N. Müller, Solid State Commun. **36**, 249 (1980).

⁷⁶O. Berger, W. Wubker, P. Mollenkamp, and J. Kessler, J. Phys. B **15**, 2473 (1982).

⁷⁷I. A. Pchelkin and G. K. Zyryanov, Prib. Tekh. Eksp., No. 6, 119 (1982).

⁷⁸M. J. M. Beerlage and P. S. Farago, J. Phys. E **14**, 928 (1981).

⁷⁹E. Kisker, Rev. Sci. Instrum. **53**, 507 (1982).

⁸⁰M. Kalisvaart, M. R. O'Neill, T. W. Riddle, F. B. Dunning, and G. K. Walters, Phys. Rev. B **17**, 1570 (1978).

⁸¹R. Feder, Surf. Sci. **51**, 297 (1975).

⁸²M. Fink, A. Yates, and J. Ingram, Atomic Data **1**, 385 (1970); **4**, 129 (1972).

⁸³W. A. Harrison, *Solid State Theory*, McGraw-Hill, New York, 1970 [Russ. Transl., Mir, M., 1972].

⁸⁴J. B. Pendry, *Low Energy Electron Diffraction*, Academic Press, London, 1974.

- don, 1974.
- ⁸⁵R. Feder, P. J. Jennings, and R. O. Jones, *Surf. Sci.* **61**, 307 (1976).
 - ⁸⁶R. Feder, *ibid.* **63**, 283 (1977).
 - ⁸⁷R. L. Calvert, G. J. Russel, and D. Hanemann, *Phys. Rev. Lett.* **39**, 1226 (1977).
 - ⁸⁸P. J. Jennings and R. O. Jones, *Surf. Sci.* **71**, 101 (1978).
 - ⁸⁹P. J. Jennings and R. O. Jones, *Solid State Commun.* **44**, 17 (1982).
 - ⁹⁰G. C. Wang, B. I. Dunlap, R. J. Celotta, and D. T. Pierce, *Phys. Rev. Lett.* **42**, 1349 (1979).
 - ⁹¹B. Reihl, M. Scharli, and M. Erbudak, *Helv. Phys. Acta* **52**, 351 (1980).
 - ⁹²R. Feder and J. Kirschner, *Surf. Sci.* **103**, 75 (1981).
 - ⁹³J. Kirschner and R. Feder, *ibid.* **104**, 448.
 - ⁹⁴K. Koike and K. Hayakawa, *Jpn. J. Appl. Phys. Part 1*, **22**, 1332 (1983).
 - ⁹⁵F. S. Marsh, M. K. Debe, and D. A. King, *J. Phys. C* **13**, 2799 (1980).
 - ⁹⁶R. Feder, *Surf. Sci.* **68**, 229 (1977).
 - ⁹⁷P. Bauer, R. Feder, and N. Müller, *ibid.* **99**, L395 (1980).
 - ⁹⁸R. Feder, H. Pleyer, P. Bauer, and N. Müller, *ibid.* **109**, 419 (1981).
 - ⁹⁹P. Bauer, W. Eckstein, and N. Müller, *Z. Phys.* **52**, 185 (1983).
 - ¹⁰⁰L. L. Kesmodel, P. C. Stair, and G. A. Somorjai, *Surf. Sci.* **64**, 342 (1967).
 - ¹⁰¹D. L. Adams, V. B. Nielsen, and M. A. van Hove, *Phys. Rev. B* **20**, 4789 (1979).
 - ¹⁰²J. A. Davies, D. P. Jackson, N. Matsunami, R. R. Norton, and J. U. Andersen, *Surf. Sci.* **78**, 274 (1978).
 - ¹⁰³N. Müller and D. Wolf, *Bull. Am. Phys. Soc.* **21**, 944 (1976).
 - ¹⁰⁴R. Feder, N. Müller, and D. Wolf, *Z. Phys. Ser. B* **26**, 265 (1977).
 - ¹⁰⁵N. Müller, D. Wolf, and R. Feder, *Instrum. Phys. Conf. Ser.* **41**, 281 (1978).
 - ¹⁰⁶R. Feder, *Surf. Sci.* **77**, 505 (1978).
 - ¹⁰⁷R. Feder, N. Müller, and D. Wolf, in: *Intern. Conference on Electron Diffraction, 1927-1977*, London, 1978.
 - ¹⁰⁸B. Reihl, *Z. Phys. Ser. B* **41**, 21 (1981).
 - ¹⁰⁹N. Müller, M. Erbudak, and D. Wolf, *Solid State Commun.* **39**, 1247 (1981).
 - ¹¹⁰M. Erbudak, G. Ravano, and N. Müller, *Phys. Lett. A* **90**, 62 (1982).
 - ¹¹¹D. G. Fedak and N. A. Gjostein, *Surf. Sci.* **8**, 77 (1967).
 - ¹¹²M. G. Lagally, J. C. Buchholz, and G. C. Wang, *J. Vac. Sci. Technol.* **12**, 213 (1975).
 - ¹¹³J. Kirschner and R. Feder, *Surf. Sci.* **79**, 176 (1979).
 - ¹¹⁴R. Feder, *Phys. Lett. A* **78**, 103 (1980).
 - ¹¹⁵B. I. Dunlap, *Solid State Commun.* **35**, 141 (1980).
 - ¹¹⁶G. Malmstrom and J. Rundgren, *J. Phys. C* **14**, 4937 (1981).
 - ¹¹⁷R. Feder, *Phys. Rev. B* **15**, 1751 (1977).
 - ¹¹⁸D. T. Pierce, R. J. Celotta, G. C. Wang, and E. G. McRae, *Solid State Commun.* **39**, 1053 (1981).
 - ¹¹⁹E. G. McRae, D. T. Pierce, G. C. Wang, and R. J. Celotta, *Phys. Rev. B* **24**, 4230 (1981).
 - ¹²⁰R. O. Jones and P. J. Jennings, *ibid.* **27**, 4702 (1983).
 - ¹²¹T. W. Riddle, A. H. Mahan, F. B. Dunning, and G. K. Walters, *Surf. Sci.* **82**, 511 (1979).
 - ¹²²J. F. Wendelken and J. Kirschner, *ibid.* **110**, 1 (1981).
 - ¹²³T. W. Riddle, A. H. Mahan, F. B. Dunning, and G. K. Walters, *ibid.* **82**, 517 (1979).
 - ¹²⁴A. H. Mahan, T. W. Riddle, F. B. Dunning, and G. K. Walters, *ibid.* **93**, 550 (1980).
 - ¹²⁵G. C. Wang, J. Unguris, D. T. Pierce, and R. J. Celotta, *ibid.* **114**, L35 (1982).
 - ¹²⁶T. W. Riddle, A. H. Mahan, F. B. Dunning, and G. K. Walters, *J. Vac. Sci. Technol.* **15**, 1686 (1978).
 - ¹²⁷L. N. Lieberman, D. R. Fredkin, and H. B. Shore, *Phys. Rev. Lett.* **22**, 539 (1969).
 - ¹²⁸C. S. Wang and A. J. Freeman, *Phys. Rev. B* **21**, 4385 (1980).
 - ¹²⁹C. S. Wang and A. J. Freeman, *J. Magn. Magn. Mater.* **15-18**, Part 2, 869 (1980).
 - ¹³⁰C. S. Wang and A. J. Freeman, *Phys. Rev. B* **24**, 4364 (1981).
 - ¹³¹O. Jepsen, J. Madsen, and O. K. Andersen, *J. Magn. Magn. Mater.* **15-18**, Part 2, 867 (1980).
 - ¹³²L. A. Vredevoe and R. E. de Wames, *Phys. Rev.* **176**, 684 (1968).
 - ¹³³X. I. Saldana and L. S. Helman, *ibid.*, Ser. B, **16**, 4978 (1977).
 - ¹³⁴R. Feder, *Phys. Status Solidi B* **58**, K137 (1973).
 - ¹³⁵R. Feder, *Solid State Commun.* **31**, 821 (1979).
 - ¹³⁶S. W. Wang, *ibid.* **36**, 847 (1980).
 - ¹³⁷S. W. Wang, R. E. Kibry, and E. L. Garvin, *ibid.* **32**, 993 (1979).
 - ¹³⁸R. Feder and H. Pleyer, *Surf. Sci.* **117**, 285 (1982).
 - ¹³⁹S. F. Alvarado, R. Feder, H. Hopster, F. Ciccacci, and H. Pleyer, *Z. Phys. Ser. B* **49**, 129 (1982).
 - ¹⁴⁰R. J. Celotta, D. T. Pierce, G. C. Wang, S. D. Bader, and G. P. Felcher, *Phys. Rev. Lett.* **43**, 728 (1979).
 - ¹⁴¹D. T. Pierce, R. J. Celotta, G. C. Wang, G. P. Felcher, S. D. Bader, and K. Miyano, *J. Magn. Magn. Mater.* **15-18**, 1583 (1980).
 - ¹⁴²S. F. Alvarado, H. Hopster, R. Feder, and H. Pleyer, *Solid State Commun.* **39**, 1319 (1981).
 - ¹⁴³S. W. Wang, *J. Appl. Phys.* **52**, 2499 (1981).
 - ¹⁴⁴S. F. Alvarado, H. Hopster, and M. Campagna, *Surf. Sci.* **117**, 294 (1982).
 - ¹⁴⁵S. F. Alvarado, M. Campagna, and H. Hopster, *Phys. Rev. Lett.* **48**, 51 (1982).
 - ¹⁴⁶S. F. Alvarado, M. Campagna, F. Ciccacci, and H. Hopster, *J. Appl. Phys.* **53**, 7920 (1982).
 - ¹⁴⁷R. Feder, S. F. Alvarado, E. Tamura, and E. Kisker, *Surf. Sci.* **127**, 83 (1983).
 - ¹⁴⁸C. E. Kuyatt, *Phys. Rev. B* **12**, 4581 (1975).
 - ¹⁴⁹J. K. Lang, K. D. Jamison, F. B. Dunning, G. K. Walters, M. A. Passler, A. Ignatiev, E. Tamura, and R. Feder, *Surf. Sci.* **123**, 247 (1982).
 - ¹⁵⁰E. Tamura and R. Feder, *Solid State Commun.* **44**, 1101 (1982).
 - ¹⁵¹G. Waller and U. Gradmann, *Phys. Rev. B* **26**, 6330 (1982).
 - ¹⁵²U. Gradmann, G. Waller, R. Feder, and E. Tamura, *J. Magn. Magn. Mater.* **31-34**, Part 2, 883 (1983).
 - ¹⁵³D. T. Pierce, R. J. Celotta, J. Unguris, and H. C. Siegmman, *Phys. Rev. B* **26**, 2566 (1982).
 - ¹⁵⁴D. T. Pierce, R. J. Celotta, and J. Unguris, *J. Magn. Magn. Mater.* **31-34**, Part 2, 869 (1983).
 - ¹⁵⁵D. T. Pierce, R. J. Celotta, *et al.*, *ibid.* **35**, 28 (1983).
 - ¹⁵⁶P. W. Palmberg, R. E. de Wames, and L. A. Vredevoe, *Phys. Rev. Lett.* **21**, 682 (1968).
 - ¹⁵⁷J. A. Walker *et al.*, *Surf. Sci.* **68**, 221 (1977).
 - ¹⁵⁸K. Namikawa, *J. Phys. Soc. Jpn.* **44**, 165 (1978).
 - ¹⁵⁹R. Feder and J. B. Pendry, *Solid State Commun.* **26**, 519 (1978).
 - ¹⁶⁰M. Erbudak and G. Ravano, *Surf. Sci.* **126**, 120 (1983).
 - ¹⁶¹L. Kleinman, *Phys. Rev. B* **17**, 3666 (1978).
 - ¹⁶²R. E. De Wames and L. A. Vredevoe, *Phys. Rev. Lett.* **18**, 873 (1967).
 - ¹⁶³D. L. Mills, *J. Phys. Chem. Solids* **28**, 2245 (1967).
 - ¹⁶⁴J. S. Helman and W. Baltensperger, *Phys. Rev. B* **22**, 1300 (1980).
 - ¹⁶⁵P. A. Wolff, *ibid.* **95**, 56 (1954).
 - ¹⁶⁶R. W. Rendell and D. R. Penn, *Phys. Rev. Lett.* **45**, 2057 (1980).
 - ¹⁶⁷A. Bringer, M. Campagna, *et al.*, *ibid.* **42**, 1705 (1979).
 - ¹⁶⁸J. A. D. Matthew, *Phys. Rev. B* **25**, 3326 (1982).
 - ¹⁶⁹S. Selzer and N. Majlis, *ibid.* **26**, 404.
 - ¹⁷⁰M. Erbudak and G. Ravano, *Phys. Lett. A* **91**, 367 (1982).
 - ¹⁷¹G. Ravano and M. Erbudak, *Solid State Commun.* **44**, 547 (1983).
 - ¹⁷²G. Ravano *et al.*, *Phys. Rev. Lett.* **49**, 80 (1982).
 - ¹⁷³J. Unguris, D. T. Pierce, A. Galejs, and R. J. Celotta, *ibid.*, p. 72.
 - ¹⁷⁴E. Kisker, R. Clauber, and W. Gudat, *Rev. Sci. Instrum.* **53**, 1137 (1982).
 - ¹⁷⁵H. Hopster, R. Raue, E. Kisker, M. Campagna, and G. Güntherodt, *J. Vac. Sci. Technol. Ser. A* **1**, Part 2, 1134 (1983).
 - ¹⁷⁶H. Hopster, R. Raue, *et al.*, *Phys. Rev. Lett.* **50**, 70 (1983).
 - ¹⁷⁷J. A. Akhiezer and E. M. Chudnovski, *Phys. Lett. A* **65**, 433 (1978).
 - ¹⁷⁸R. Reifenberger and M. J. G. Lee, *Transition Metals (Inst. of Physics Conf. Ser.)* Toronto, 1977.
 - ¹⁷⁹H. M. Klar, *J. Phys. B* **3**, 4741 (1980).
 - ¹⁸⁰N. Kabachnik, *ibid.* **14**, L337 (1981).
 - ¹⁸¹K.-N. Huang, *Phys. Rev. A* **26**, 2274 (1982).
 - ¹⁸²M. Landolt and D. Mauri, *Phys. Rev. Lett.* **49**, 1783 (1982).
 - ¹⁸³D. P. Woodruff, N. Y. Smith, P. D. Jonson, and W. A. Royer, *Phys. Rev. B* **26**, 2943 (1982).
 - ¹⁸⁴J. Unguris, A. Seiler, R. J. Celotta, *et al.*, *Phys. Rev. Lett.* **49**, 1047 (1982).
 - ¹⁸⁵C. Rau and S. Eichner, *ibid.* **47**, 939 (1981).
 - ¹⁸⁶C. Rau, *Appl. Surf. Sci.* **13**, 310 (1982).
 - ¹⁸⁷P. W. Zitzewitz *et al.*, *Phys. Rev. Lett.* **43**, 1281 (1979).
 - ¹⁸⁸R. Feder, *Solid State Commun.* **34**, 541 (1980).

Translated by M. V. King